

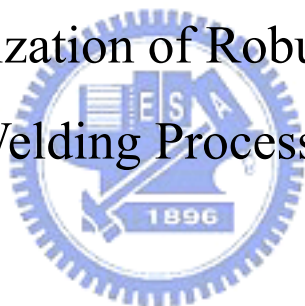
國立交通大學

機械工程學系

博士論文

銲接製程穩健設計最佳化之研究

Study on Optimization of Robust Design for the  
Welding Processes



研究生：林玄良

指導教授：周長彬

中華民國九十五年十二月

銲接製程穩健設計最佳化之研究

Study on Optimization of Robust Design for the  
Welding Processes

研究生：林玄良

Student：Hsuan-Liang Lin

指導教授：周長彬

Advisor：Chang-Pin Chou

國立交通大學



A Thesis

Submitted to Institute of Mechanical Engineering

College of Engineering

National Chiao Tung University

in Partial Fulfillment of the Requirements

for the Degree of

Doctor of Philosophy

in

Mechanical Engineering

December 2006

Hsinchu, Taiwan, Republic of China

中華民國九十五年十二月

# 銲接製程穩健設計最佳化之研究

研究生：林玄良

指導教授：周長彬

國立交通大學機械工程學系

## 摘要

在自動化銲接的製程領域中，影響銲接品質的參數頗多。在銲接實務上，製程參數一般根據過去的經驗，或是參考文獻資料及設備供應商建議的數據來決定。對於特定的銲接系統或環境條件，此方式難以確保可得到最佳化的銲接品質。一般業界使用田口方法解決上述問題，然而田口方法在實務應用上存在一些缺失。由於應用田口方法於類神經網路設計，可得到許多網路設計的效益，因此，本論文提出一結合田口方法與類神經網路的方法，以改善參數設計最佳化的銲接問題。此方法包括二階段，階段一利用田口方法針對銲接製程執行初始最佳化的實驗，以建立後續訓練類神經網路的資料庫。階段二應用類神經網路來搜尋最佳的參數組合，並採用 Levenberg-Marquardt 倒傳遞演算法。本論文利用三個銲接的實務案例，包括氣體鎢極電弧銲、脈衝式 Nd:YAG 雷射微接合及汽車電阻點銲等製程，來說明所提方法的有效性。實驗結果顯示本論文所提的方法優於傳統應用田口方法；氣體鎢極電弧銲接平均可提昇 11.96% 的銲道深寬比，脈衝式 Nd:YAG 雷射微接合可降低 3.37% 的不良品率，電阻點銲平均可提昇 7.26% 的拉剪強度值；由此實務操作及結果，可說明所提方法具備高度的可行性。

# Study on Optimization of Robust Design for the Welding Processes

Student : Hsuan-Liang Lin

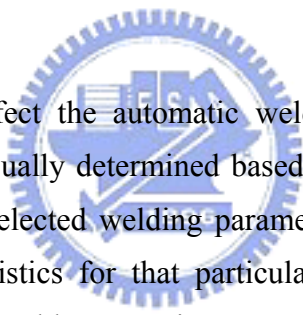
Advisor : Chang-Pin Chou

Department of Mechanical Engineering

College of Engineering

National Chiao Tung University

## ABSTRACT



Many parameters affect the automatic welding quality. In practice, the desired welding parameters are usually determined based on experience or handbook values. It does not insure that the selected welding parameters result in optimal or near optimal welding quality characteristics for that particular welding system and environmental conditions. To solve such problems, engineers conventionally apply the Taguchi method. However, the Taguchi method has some limitations in practice. Many benefits can arise from using the Taguchi method for neural network design. A proposed approach that combine the Taguchi method and a neural network to determine optimal welding conditions for improving the effectiveness of the optimization of parameter design is presented. The proposed approach includes two phases. Phase 1 executes initial optimization via Taguchi method to construct a database for the neural network. Phase 2 applies a neural network with the Levenberg-Marquardt back-propagation (LMBP) algorithm to search for the optimal parameter combination. Three examples involving the gas tungsten arc (GTA) welding, the pulsed Nd:YAG laser micro-weld process, and the resistance spot welding (RSW) process in automotive industry demonstrate the effectiveness of the proposed approach. The experimental results show that the proposed procedures excel the Taguchi method in this dissertation. It has demonstrated the practicability of the proposed procedures.

## ACKNOWLEDGEMENT

首先要感謝指導教授周長彬博士的悉心教誨與策勵支持，使本篇論文得以順利完成。師恩浩瀚，學生必定永銘於心。

口試期間，承蒙林義成教授、鄭璧瑩教授、紀勝財教授、鄭慶民教授及李義剛博士等委員，對本篇論文的研究架構與文字編排等細心地審閱、斧正，使論文內容更臻於完備，謝謝您們。研究期間，交大電控系周志成教授及清大工工系蘇朝墩教授，在類神經網路及品質工程等課程的認真講授與問題釋疑，讓學生獲益良多，在此致上最誠摯的謝意；感謝鈦思科技吳榮鴻先生提供類神經網路軟體，碩士專班蔡勝禮及周定，提供雷射微接合設備，及汽車鋼板電阻點鐸設備。另外，碩士班指導教授邱弘興博士在田口方法的啟蒙，並為我撰寫推薦函，使我能順利進入交大機械系攻讀博士學位，在此一併向您表達最誠摯的謝意。

感謝學長曾光宏博士及同學黃和悅博士，在實驗研究與國際期刊投稿之經驗傳承，實驗室的師兄弟林后堯、蔡曜隆、林國書、徐享文、郭承憲、羅仁聰、林志光、張佑銘及溫華強等，在課業及研究工作方面的相互切磋、交流及砥礪。另外，要感謝黃處明、蔡勝禮、黃泰勳、周定及陳明松等，在合作實驗研究期間認真、努力地付出。感謝陸軍專科學校車輛工程科的全體同仁，在這段攻讀學位的日子裡，能與您們一同愉快地工作，分享、交流作研究的心得，並能得到您們全心全意的協助，謝謝您們的厚愛。

感謝父母的養育之恩與用心栽培，兄長們的支持與鼓勵，及岳母盡心盡力地照顧兩個頑皮兒子，您們無怨無悔的付出，使我無後顧之憂，得以安心地完成學位。要特別感謝的是愛妻淑雯，您對家庭的付出及對昱穎、昱緯的悉心照護，給我莫大的自由度倘佯在研究的領域中，您是我能夠順利完成博士學業的最大原動力，謝謝您。最後，僅以此論文獻給曾經幫助過我、關心我的人，謝謝您們。

# TABLE OF CONTENTS

ABSTRACT (IN CHINESE).....	i
ABSTRACT .....	ii
ACKNOWLEDGEMENT.....	iii
TABLE OF CONTENTS .....	iv
LIST OF TABLES.....	vi
LIST OF FIGURES .....	viii
<b>CHAPTER 1 INTRODUCTION .....</b>	<b>1</b>
1.1 Backgrounds.....	1
1.2 Motivation.....	2
1.3 Objectives.....	3
1.4 Dissertation Outlines.....	3
<b>CHAPTER 2 LITERATURE REVIEW .....</b>	<b>5</b>
2.1 Taguchi Method .....	5
2.2 Neural networks .....	9
2.3 Integrated the Taguchi method and a neural network .....	16
2.4 The gas tungsten arc (GTA) welding .....	17
2.5 Nd:YAG laser micro-weld .....	20
2.6 Resistance spot welding (RSW) in automotive industry.....	24
<b>CHAPTER 3 EXPERIMENTAL PROCEDURES .....</b>	<b>27</b>
3.1 Proposed procedure .....	27

3.2 Optimization for GTA welding.....	28
3.2.1 Initial optimization for GTA welding.....	28
3.2.2 Real optimization for GTA welding .....	39
3.3 Optimization for Nd:YAG laser micro-weld .....	42
3.3.1 Initial optimization for Nd:YAG laser micro-weld .....	42
3.3.2 Real optimization for Nd:YAG laser micro-weld.....	54
3.4 Optimization for RSW process.....	61
3.4.1 Initial optimization for RSW process.....	61
3.4.2 Real optimization for RSW process .....	70
<b>CHAPTER 4 RESULTS AND DISCUSSION.....</b>	<b>77</b>
4.1 Experimental results of GTA welding.....	77
4.2 Experimental results of Nd:YAG laser micro-weld.....	79
4.3 Experimental results of RSW process .....	81
<b>CHAPTER 5 CONCLUSION .....</b>	<b>84</b>
<b>REFERENCE.....</b>	<b>86</b>
<b>AUTHOR’S PUBLICATION LIST.....</b>	<b>91</b>

## LIST OF FIGURES

Fig.2-1	Schematic of measurement for weld pool geometry .....	19
Fig.2-2	Cause and effect diagram of the GTA welding process.....	19
Fig.2-3	Lithium-ion secondary battery and its micro-weld position	22
Fig.2-4	Testing instrument and the schematic of measurement .....	23
Fig.2-5	Cause and effect diagram of the Nd:YAG laser welding ...	24
Fig.2-6	Universal testing machine used .....	26
Fig.3-1	The equipment of Autogenous GTA welder .....	29
Fig.3-2	Measurement of weld pool geometry.....	33
Fig.3-3	S/N graph for the weld pool geometry.....	37
Fig.3-4	The BP network topology of the GTA welding process.....	41
Fig.3-5	Simulation different electrode angle and welding current ...	42
Fig.3-6	Pulsed Nd:YAG laser spot welder .....	43
Fig.3-7	Illustration of automatic production .....	44
Fig.3-8	SNR graph for the quality characteristic.....	51
Fig.3-9	The BP network topology of the Nd:YAG laser welding ...	56
Fig.3-10	Results of simulating different pulse width.....	57
Fig.3-11	Results of simulating different focus position.....	58
Fig.3-12	Results of simulating different pulse frequency.....	59
Fig.3-13	Results of simulating different pulse peak value.....	60
Fig.3-14	Schematic diagram of the specimens.....	61
Fig.3-15	Resistance spot welder and prepared specimens.....	62
Fig.3-16	SNR graph for the Max. Load.....	67



Fig.3-17	The BP network topology of the RSW process .....	72
Fig.3-18	Results of simulating different welding time .....	73
Fig.3-19	Results of simulating different electrode force .....	74
Fig.3-20	Results of simulating different size of the electrode tip.....	75
Fig.3-21	Results of simulating different welding current.....	76
Fig.4-1	Weld pool geometry for validation.....	78
Fig.4-2	Surface conditions of specimens for validation .....	83



## LIST OF TABLES

Table 2-1	Parameters for GTA welding .....	18
Table 2-2	Parameters for laser welding.....	21
Table 3-1	Material used in GTA welding (wt-%).....	28
Table 3-2	Control factors of GTA welding .....	30
Table 3-3	Experimental layout using an $L_{27}$ orthogonal array .....	32
Table 3-4	Summary of experiment data of GTA welding.....	35
Table 3-5	<i>S/N</i> response table for the weld pool geometry .....	36
Table 3-6	Results of ANOVA for the weld pool geometry .....	38
Table 3-7	Confirmation experiment of GTA welding .....	39
Table 3-8	Options for different networks in GTA welding .....	40
Table 3-9	Material used in Nd:YAG laser spot welding (wt-%) .....	43
Table 3-10	Control factors of Nd:YAG laser spot welding.....	46
Table 3-11	Experimental layout using $L_{25}$ orthogonal array .....	48
Table 3-12	Experiment data of Nd:YAG laser micro-weld.....	50
Table 3-13	SNR response table for the quality characteristic.....	51
Table 3-14	Results of ANOVA for the quality characteristic.....	52
Table 3-15	Confirmation experiment of Nd:YAG laser micro-weld...	53
Table 3-16	Options for different networks in Nd:YAG laser welding	55
Table 3-17	Material used in RSW process.....	61
Table 3-18	Control factors of RSW process .....	63
Table 3-19	Experimental layout using an $L_{16}$ orthogonal array .....	64
Table 3-20	Experiment data of RSW process.....	65

Table 3-21	SNR response table for the Max. Load.....	67
Table 3-22	Results of ANOVA for the Max. Load.....	68
Table 3-23	Confirmation experiment of RSW process .....	69
Table 3-24	Results of the Taguchi method with proper regulation.....	70
Table 3-25	Options for different networks in RSW process .....	71
Table 4-1	Results of the proposed approach in GTA welding.....	77
Table 4-2	Results of the proposed approach in laser welding .....	79
Table 4-3	A comparison of each condition .....	80
Table 4-4	Results of the proposed approach in RSW process .....	82
Table 4-5	Results of the initial conditions in RSW process.....	82



# CHAPTER 1

## INTRODUCTION

### 1.1 Backgrounds

Welding is the most efficient way to join metals. It involves more sciences and variables (parameters) than other industrial process. Welding is widely used to manufacture or repair all products made of metal. Look around, almost everything made of metals is welded; such as automobiles, ships, airplanes, bridges, buildings, home appliances, microelectronic appliances and so on.

Welding is an economical manufacturing method. In the high-volume production industries it is common to see welding operations intermixed with bending, machining, forming and assembly. Welding is an important manufacturing process taking its place with other metalworking operations to produce high quality metal products at economical prices.

The recent trends in the welding and manufacturing it becomes evident that the following must be considered with regard to the future welding [1]:

1. There will be a continuing need to reduce manufacturing cost since:
  - a. Wage rates will continue to increase.
  - b. The cost of metals and filler metals will continue to be more expensive.
  - c. Energy and fuel costs will increase.
2. There will be a continuing trend toward the use of higher strength

materials.

3. There will be more use of welding by industry, decreasing the use of casting.
4. There will be a continuing trend toward higher levels of reliability and higher-quality requirements.
5. The trend toward automatic welding and automation in welding will accelerate.

## **1.2 Motivation**

There are many parameters that affect the automatic welding quality such as the gas tungsten arc (GTA) welding, the laser welding, and the resistance spot welding (RSW) in automotive industry. In practice, the desired welding parameters are usually determined based on experience or handbook values. It does not insure that the selected welding parameters result in optimal or near optimal welding quality characteristics for that particular welding system and environmental conditions.

The Taguchi method, a popular experimental design method applied in industry, can alleviate on the disadvantages of full factorial design when doing fractional factorial design. It approaches the optimization of parameter design, although the number of experiments is reduced [2]. However, the Taguchi method has certain limitations when used in practice. The optimal solutions were only obtained within the specified level of control factors. Once the parameter setting is determined, the range of optimal solutions is constrained concurrently. The Taguchi method is unable to find the real optimal values when the specified parameters are continuous in nature, because it only addresses the discrete control factors.

Neural network is a non-linear function, capable of accurately representing a complex relationship between inputs and outputs [3-5]. The trained neural model was also used to accurately predict the response at given parameter settings. In addition, Khaw *et al.* [6] proved that benefits could be obtained by using the Taguchi concept for neural network design. First, this methodology is the only known method for neural network design that considers robustness. It enhances the quality of the neural network designed. Second, the Taguchi method uses orthogonal arrays (OAs) to systematically design a neural network. Subsequently, the design and development time for neural networks can be reduced tremendously.

### **1.3 Objectives**

This dissertation employs an approach, which combine the Taguchi method and a neural network to determine optimal conditions for improving the welding process quality. Three welding processes are focus in this dissertation:

1. Optimization of the gas tungsten arc (GTA) welding process for type 304 stainless steels.
2. Modeling and optimization of the Nd:YAG laser micro-weld for the lithium-ion secondary batteries.
3. Modeling and optimization of the resistant spot welding (RSW) process for high strength steel sheets in automotive industry.

### **1.4 Dissertation outlines**

Chapter 2 reviews that the Taguchi method, neural networks, combined Taguchi method with a neural network, the GTA welding for type 304

stainless steels, the pulsed Nd:YAG laser micro-weld for the lithium-ion secondary batteries, and RSW process for high strength steel sheets in automotive industry. Chapter 3 presents that the proposed approach was used to determine optimal conditions for improving process quality of the GTA welding, the pulsed Nd:YAG laser micro-weld and RSW process. In addition, this chapter presents the initial optimization via Taguchi method, and a neural network with the Levenberg-Marquardt back-propagation (LMBP) algorithm to search for the optimal parameter combination for these welding processes. Chapter 4 provides the discussion comparison with previous works and the proposed procedures. Finally, Chapter 5 concludes the main results of the presented work.



# **CHAPTER 2**

## **LITERATURE REVIEW**

### **2.1 Taguchi method**

The philosophy of Taguchi is broadly applicable. It considers three stages in process development: system design, parameter design and tolerance design [2,7]. In system design, the engineer uses scientific and engineering principles to determine the basic configuration. The main objective of system design is to determine the manufacturing process that can produce the product within the specified limits and tolerance at the lowest cost. In the parameter design stage, specific values for the system parameters are determined. Parameter design in production process design determines the operating levels of the manufacturing processes so that variation in product parameters is minimized. Tolerance design is used to specify the best tolerances for the parameters. The objective of tolerance design is to find optimal ranges of the operating conditions that minimize the sum of variation cost and cost of the product.

In addition, traditional experimental design is primarily used to improve the average level of a process (e.g., arithmetic mean of a sample). In modern quality engineering, experimental design work is used to develop robust designs to improve the quality of the product. Taguchi's parameter design is to achieve robust quality by reducing effects of environmental conditions and variations caused by deterioration of certain components [7,8]. This is achieved by the selection of various design alternatives or by varying the levels of the design parameters for component parts or system elements. It can optimize the performance characteristics through the settings of design parameters and reduce the sensitivity of the system performance to sources of variation.



The tools for executing the parameter design oh Taguchi method are shown as below [7-10]:

### ***Orthogonal array***

Orthogonal array (OA) based matrix experiments are used for a variety of purposes in Robust Design. They are used to study the effects of control factors and noise factors, and determine the best quality characteristic for particular applications. Taguchi has tabulated 18 basic orthogonal arrays that are called standard OAs. Note that the orthogonality was preserved even when the dummy level technique was applied to one or more factors. In addition, the noise factor could be assigned to the outer array to find some level of a control factor that does not have much variation in the results, even though a noise factor is definitely present.



### ***Evaluation by S/N ratios***

Taguchi has created a transformation of the repetition data to another value, which is to say a measure of the variation present. The transformation is the signal-to-noise ratio (S/N ratio, SNR). There are several S/N ratios available depending on the type characteristic being present, such as lower-is-better (LB), nominal-is-best (NB), or higher-is-better (HB).

For a static problem, Taguchi classified them into three different S/N ratio types, as shown in equation 2-1, 2-2 and 2-3.

$$SN_{NB} = -10 \log_{10} \left( \frac{\bar{y}}{s} \right)^2 \quad 2-1$$

$$SN_{LB} = -10 \log_{10} \left( \frac{1}{n} \sum_{i=1}^n \frac{1}{y_i^2} \right) \quad 2-2$$

$$SN_{SB} = -10 \log_{10} \left( \frac{1}{n} \sum_{i=1}^n y_i^2 \right) \quad 2-3$$

were  $n$  denote the number of repetition,  $\bar{y}$  represents the response mean, and  $s$  is the standard deviation of response.

### ***Analysis of variance***

The Analysis of Variance (ANOVA) was developed by Sir Ronald Fisher in the 1930's as a way to interpret the results from agricultural experiments. ANOVA is not a complicated method and has a large amount of mathematical uniqueness associated with it. The purpose of the ANOVA is to investigate welding process parameters, which can significantly affect the quality characteristics. The percent contribution in the total sum of the squared deviations can be used to evaluate the importance of the welding process parameter change on these quality characteristics. In addition, the F-Test named after Fisher can also be used to determine which welding process parameters have a significant effect on the quality characteristics. Usually, when the value of F-Test is greater than 4, it means that a change in the process parameter has a significant effect on the quality characteristics. When the contribution of a factor is small, the sum of squares for that factor is combined with the error. This process of disregarding the contribution of a selected factor and subsequently adjusting the contributions of the other factors is known as "Pooling".

### ***Confirmation tests***

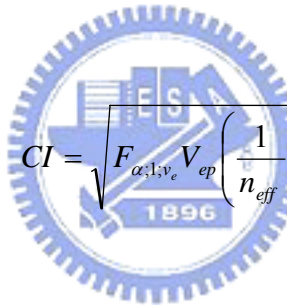
Using the Taguchi method for parameter design, the predicted optimum setting need not correspond to one of the rows of the matrix experiment. Therefore, the final step is to compare the estimated value with the confirmative experimental value using the optimal level of the control factors to confirm with

the experimental reproducibility. The estimated S/N ratio  $\eta_{opt}$  using the optimal level of the control factors can be calculated as:

$$\eta_{opt} = \hat{\eta} + \sum_{j=1}^q (\eta_j - \hat{\eta}) \quad 2-4$$

where  $\hat{\eta}$  is the total average of S/N ratio of all the experimental values,  $\eta_j$  is the mean S/N ratio at the optimal level, and  $q$  is the number of the control factors that significantly affect the quality characteristic.

The confidence interval is a maximum and minimum value between which the true average should fall at some stated percentage of confidence. The confidence limits of the above estimation can be calculated taking into account the following equation:



$$CI = \sqrt{F_{\alpha;1;v_e} V_{ep} \left( \frac{1}{n_{eff}} + \frac{1}{r} \right)} \quad 2-5$$

where  $F_{\alpha;1;v_e}$  is the F-ratio required for  $\alpha$ =risk, confidence=1 – risk,  $v_e$  is the degrees of freedom for pooled error,  $V_{ep}$  is the pooled error variance,  $r$  the sample size for the confirmation experiment, and  $n_{eff}$  is the effective sample size:

$$n_{eff} = \frac{N}{1 + DOF_{opt}} \quad 2-6$$

where  $N$  is the total number of trials,  $DOF_{opt}$  is the total degrees of freedom associated with items used in the  $\eta_{opt}$  estimate.

### ***Apply Taguchi method to welding processes***

Juang *et al.* [11] presented a study that application of Taguchi method to select parameters for obtaining an optimal weld pool geometry in the GTA welding of stainless steel. In this study, a weighting method is used to integrate the loss functions into the overall loss function (the higher-is-better of S/N ratio); the weighting factors for the front height and back height of the weld pool were selected as 0.4, the weighting factors for the front width and back width of the weld pool were selected as 0.1.

Li *et al.* [12] using the RSW process as an example, this paper presents a new robust design and analysis framework for products and processes with parameter interdependency. The experiment was designed using a two-stage, sliding-level factor approach. Welding current was chosen as a “slide factor” whose settings are determined based on those of others including both control and noise factors. By proper coding, a stepwise regression procedure was used to develop a response model, with which the response modeling approach for robust design is applied.

Tarng *et al.* [13] used grey-based Taguchi method for the optimization of the submerged arc welding (SAW) process parameters in hardfacing with considerations of multiple weld qualities. In this approach, the grey relational analysis was used as the performance characteristic in the Taguchi method. Then, optimal process parameters were determined by using the parameter design proposed by the Taguchi method.

## **2.2 Neural networks**

Neural networks are used for modeling of complex manufacturing processes, usually with regard to process and quality control [14,15]. Several

well known supervised learning networks use a back propagation (BP) neural network. Funahashi [16] proved that the BP neural network may approximately realize any continuous mapping. Back propagation learning employs a gradient descent algorithm to minimize the mean square error between the target data and the predictions of a neural network. However, one of the major problems with basic BP algorithm (gradient descent algorithm) has been the extended training time required. The techniques for accelerating convergence have fallen into two main categories: heuristic methods and standard numerical optimization methods such as the Levenberg-Marquardt back-propagation (LMBP) algorithm [17].

### ***Levenberg-Marquardt back-propagation algorithm***

The LMBP algorithm is similar to the quasi-Newton method, in which a simplified form of the Hessian matrix (second derivatives) is used. Starting from the Taylor series approach of second order, for a generic function  $F(x)$ , the following can be written [17-19].

$$F(x_{k+1}) = F(x_k + \Delta x_k) \cong F(x_k) + G(x, k)\Delta x_k + \frac{1}{2}\Delta x_k H(x, k)\Delta x_k \quad 2-7$$

Where  $G(x, k)$  is the gradient of  $F(x)$ ,  $\Delta x_k$  is  $x_{k+1} - x_k$  and  $H(x, k)$  is the Hessian matrix of  $F(x)$ .

If the derivative of equation 2-4 in respect to  $\Delta x_k$  is taken, equation 2-8 will be obtained.

$$G(x, k) + H(x, k)\Delta x_k = 0 \quad 2-8$$

This equation can be re-written in the following form.

$$\Delta x_k = -H(x, k)^{-1} G(x, k) \quad 2-9$$

The updating rule for the Newton algorithm is then obtained.

$$x_{k+1} = x_k - H(x, k)^{-1} G(x, k) \quad 2-10$$

Considering a generic quadratic function as the objective function, as represented in equation 2-11 for a multi-input multi-output system (here the iteration index is omitted and  $i$  is the index of the outputs)

$$F(x) = \sum_{i=1}^N e_i^2(x) \quad 2-11$$

Then it can be shown that

$$G(x) = J^T(x)e(x) \quad 2-12$$

$$H(x) = J^T(x)J(x) + S(x) \quad 2-13$$

Where  $J(x)$  is the Jacobian matrix and  $S(x)$  is

$$S(x) = \sum_{i=1}^N e_i(x) \nabla^2 e_i(x) \quad 2-14$$

It can be assumed that  $S(x)$  is small when compared to the product of the Jacobian, the Hessian matrix can be approximated by the following.

$$H(x) \approx J^T(x)J(x) \quad 2-15$$

This approach can update equation 2-10 and gives the Gauss-Newton algorithm.

$$\Delta x_k = [J^T(x)J(x)]^{-1} J^T(x)e(x) \quad 2-16$$

One limitation that can happen with this algorithm is that the simplified Hessian matrix might not be invertible. To overcome this problem, a modified Hessian matrix can be used.

$$Hm(x) = H(x) + \mu I \quad 2-17$$

Here  $I$  is the identity matrix and  $\mu$  is a value such that makes  $Hm(x)$  positive definite, and therefore can be invertible. This last change in the Hessian matrix corresponds to the Levenberg-Marquardt algorithm.

$$\Delta x_k = [J^T(x)J(x) + \mu I]^{-1} J^T(x)e(x) \quad 2-18$$

When the scalar  $\mu$  is zero, this is just Gauss-Newton, using the approximate Hessian matrix. When  $\mu$  is large, this becomes gradient descent with a small step size. The algorithm begins with  $\mu$  set to some small value (e.g.  $\mu=0.01$ ). If a step does not yield a smaller value for  $e$ , then the step is repeated with  $\mu$  multiplied by some factor  $\theta > 1$  (e.g.  $\theta=10$ ). Eventually  $e$  should be decreased, since we would be taking a small step in the direction of steepest descent. If a step does produce a smaller value for  $e$ , then  $\mu$  is divided by  $\theta$  for the next step, ensuring that the algorithm will approach Gauss-Newton, which should provide faster convergence [17].

The LMBP algorithm is the fastest algorithm that has been tested for

training multiplayer networks of moderate size, even though it requires a matrix inversion at each iteration. It requires two parameters, but the algorithm does not appear to be sensitive to this selection. In addition, Kumar et al. proved [20] that the LMBP algorithm and Gauss-Newton were found to perform best for least square problems. In particular, the LMBP algorithm performs better with a poor initial estimate compared to the Gauss-Newton method. Summary, the LMBP algorithm provides a nice compromise between the speed of Newton's method and the guaranteed convergence of steepest descent.

### ***Training of back propagation Network***

A neural network, which can capture and represent the relationship between the process variables and process outputs, was developed in this stage. Multi-layer perceptions are feed-forward neural networks are commonly used for solving difficult predictive modeling problems [21]. They usually consist of an input layer, one or more hidden layers, and one output layer. The neurons in the hidden layers are computational units that perform non-linear mapping between inputs and outputs. A feed-forward neural network was used in this study. The transfer functions for all hidden neurons are a tangent sigmoid function as shown in equation 2-19. The transfer functions for the output neurons are a linear function as shown in equation 2-20 [22].

$$f(x) = \frac{\exp(x) - \exp(-x)}{\exp(x) + \exp(-x)} \quad 2-19$$

$$f(x) = x \quad 2-20$$

Determining the number of hidden neurons is critical in the design of neural network. An over abundance of hidden neurons give too much flexibility



that usually leads to over-fitting. On the other hand, too few hidden neurons restrict the learning capability of a network and degrade its approximation performance [21].

### ***Apply neural networks to welding processes***

Kim *et al.* [23] develop an intelligent system in gas metal arc (GMA) welding process using MATLAB/SIMULINK software. Based on multiple regressions and a neural network, the mathematical models were derived from extensive experiments with different welding and complex geometrical features. In this study, using a generalized least mean square (LMS) algorithm, the BP algorithm minimizes the mean square difference between the real and the desired output. The developed neural network model can proposed for real-time quality control based on observation of bead geometry and for on-line welding process control. However, it was trained for 200,000 iterations.

Wu *et al.* [24] present a study that introduces a Kohonen network (self-organising feature map) system for process monitoring and quality evaluation in GMA welding. The Kohonen network is an unsupervised learning neural network. It can be used to solve classification tasks and to find structures in data. In the present study the evaluation gives a rather high recognition rate.

Nagesh *et al.* [25] used a neural network with basic BP algorithm (gradient descent algorithm) to model the shielded metal-arc welding process. The trained neural network model had achieved good agreement with the training data and had yielded satisfactory generalization. It was trained for 11,000 iterations.

Ridings *et al.* [26] present a study that describes the application of neural network techniques to the prediction of the outer diameter weld bead shape for

three wire, single pass per side, submerged arc, linepipe seam welds, using the weld process parameters as inputs. This study show that the use of neural network models for the prediction of weld bead geometry has the potential for a detailed shape to be input into through process models, rather than having to assume a shape from a limited number of defining parameters.

Jeng *et al.* [27] adopted two back-propagation (BP) and one learning vector quantization (LVQ) neural network models to predict the laser welding parameters and the associated welding quality individually, because some of the parameters are strongly interconnected and must be determined by sequence. LVQ is a supervised learning technique that uses class information to move the classification set slightly, so as to improve the quality of the classifier decision region.

Lee *et al.* [28] employed multiple regression analysis and neural network to predict the back-bead of geometry in the GMA welding process. The neural network showed superior results to the multiple regression analysis in terms of field of prediction error rate.

Vitek *et al.* [29] present a welding process that combined plasma arc welding with laser welding was used to make autogenous bead on plate welds on a sheet stock of a carbon steel. The predictions of the neural network model showed excellent agreement with experiment results, indicating that a neural network model is a viable means for predicting weld pool shape. Thirty-three different experimental welds were made. These welds provide a total data set of 33 weld conditions and the corresponding weld pool shape. It was subdivided into 11 train/test pairs consisting of 30 and 3 data points respectively.

Tarng *et al.* [30] used a neural network to construct the relationships between welding process parameters and weld pool geometry in GTA welding.

An optimization algorithm called simulated annealing was then applied to the network for searching the process parameters with an optimal weld pool geometry. The quality aluminum welds based on the weld pool geometry was classified and verified by a fuzzy clustering technique. In this study, cleanliness of specimens was selected as the input of BP network model.

Han [31] used a neural network to obtain the knowledge about the fatigue lives of weldments with welding defects under fatigue load. A total data set of 15 conditions and the corresponding fatigue life. It was divided into train and test pairs consisting of 10 and 5 data points respectively.

### **2.3 Integrated the Taguchi method and a neural network**

Rowlands *et al.* [32] present a study that illustrate how optimal parameter design can be achieved by using design of experiments in conjunction with neural network. Applying the method, the neural network was trained by the results of a fractional factorial design, and was then used to estimate the response values for the full factorial design.

Chiu *et al.* [33] used the neural network model and the Taguchi method to determine the optimal parameter setting in a gas-assisted injection molding. The results showed that the integrated method is capable of treating continuous parameter values.

Khaw *et al.* [6] proved that benefits could be obtained by using the Taguchi concept for neural network design. First, this methodology is the only known method for neural network design that considers robustness. It enhances the quality of the neural network designed. Second, the Taguchi method uses orthogonal arrays (OAs) to systematically design a neural network. With the effective use of the Taguchi method, several important design factors of a neural

network can be considered simultaneously. The design and development time for neural networks can be reduced tremendously. The Taguchi method is not strictly confined to the design of BP neural networks. It can be used to evaluate neural networks of different types such as counter-propagation, Boltzmann machine, and self-organizing map.

#### **2.4 The gas tungsten arc (GTA) welding**

The GTA welding is an arc welding process that uses an arc between a tungsten electrode (non-consumable) and the weld pool. The process is used with shielding gas and without the application of pressure for pieces to be welded. GTA welding was originally developed for aluminum and stainless steel that are difficult to be welded. The GTA welding process is now widely used with other alloys. The aircraft industry is one principal users of GTA welding [1]. There are many parameters that affect the GTA welding quality, such as electrode type, shielding gas type, welding current, travel speed of the welding torch and so forth.

GTA welding and related processes are capable of producing very high-quality welds but for consistent results the influence of the welding parameters on weld geometry and quality must be identified and controlled [34]. In conventional DC GTA welding, the main control parameters are shown in Table 2-1. The desired welding parameters are usually determined based on experience or handbook values. However, it does not insure that the selected welding parameters result in optimal or near optimal welding quality characteristics for that particular welding system and environmental conditions.

Table 2-1 Parameters for GTA welding

Primary	Secondary
Current	Arc length
Travel speed	Polarity
	Shielding gas
	Electrode vertex angle
	Filler addition



***Quality characteristic of the GTA welding process***

Basically, the GTA welding quality is strongly characterized by the weld pool geometry. The weld pool geometry plays an important role in determining the mechanical properties of the weld [25,35-36]. The measurements of the weld pool geometry were performed for evaluating the quality of GTA welds. The width of weld bead and the depth of penetration are used to describe the weld pool geometry, as shown in Fig.2-1.

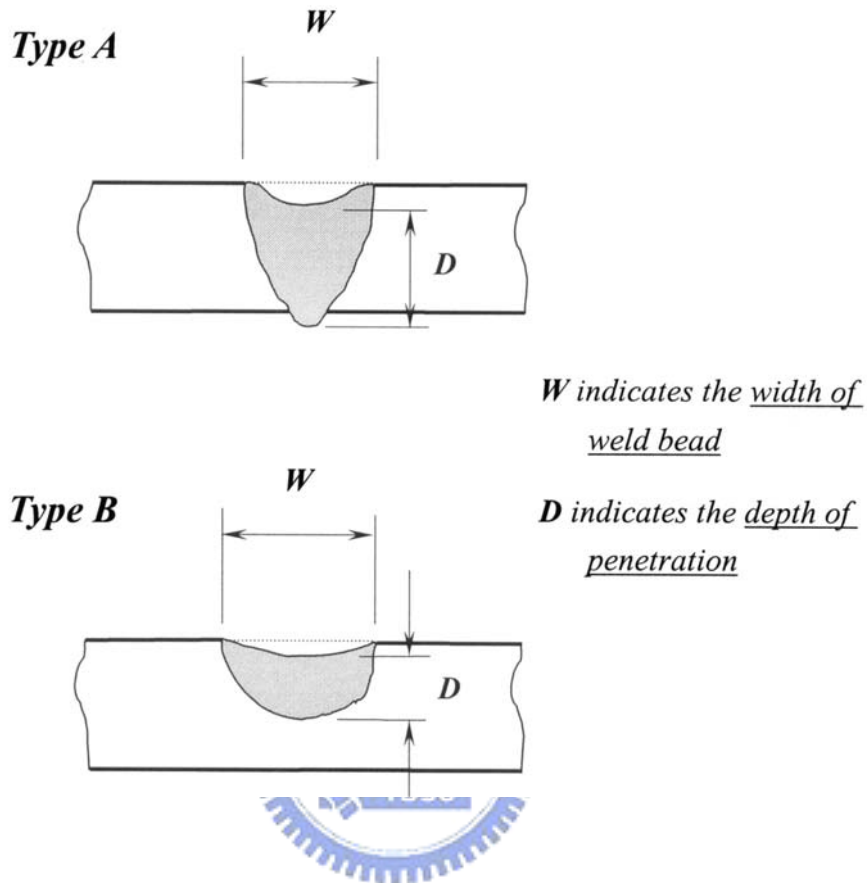


Fig.2-1 Schematic of measurement for weld pool geometry

### ***Parameters of the GTA welding process***

Several methods are useful in determining which factors to include in the initial experiments such as brainstorming, flowcharting, and cause-effect diagram [7]. Fig.2-2 is the cause-effect diagram of this process.

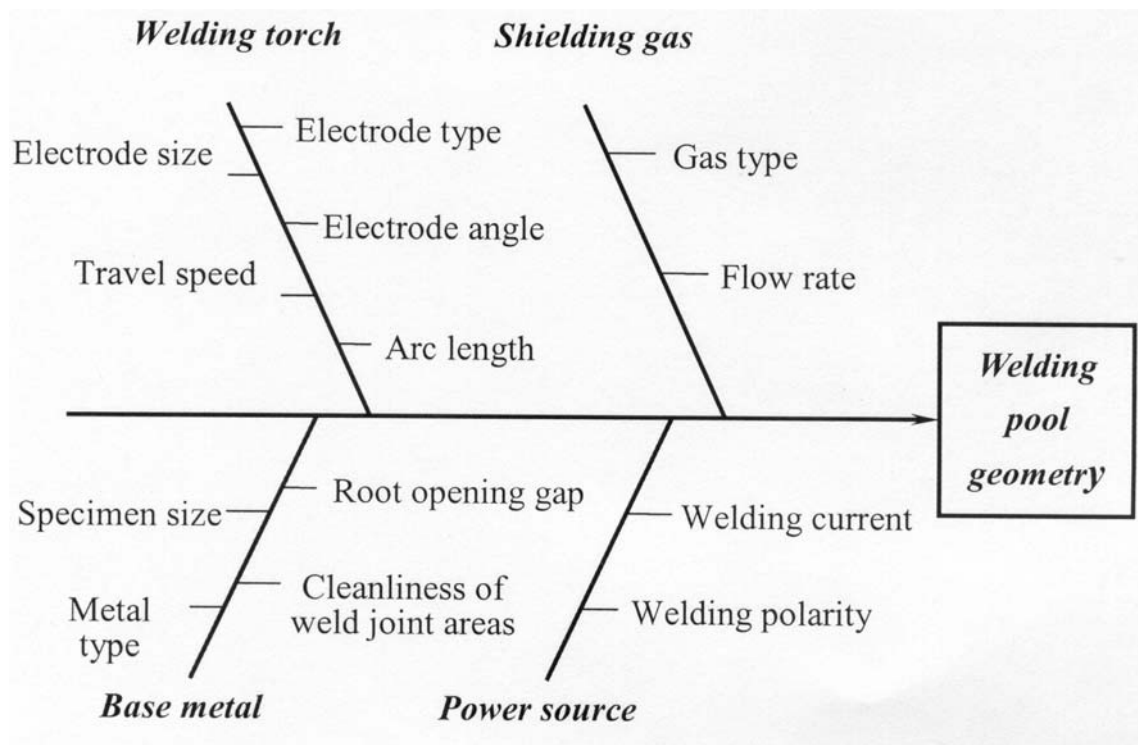


Fig.2-2 Cause and effect diagram of the GTA welding process

## 2.5 Nd:YAG laser micro-weld

In the mass production process of lithium-ion secondary batteries, the lap-weld process of safety vent and cathode lead is the major factor to affect product quality and production efficiency. The laser spot welding is the micro-joining technique most frequently used in the electron related industry. Spot welding was the first welding operation to be carried out with lasers. The higher-pulse repetition rates and pulse-tailoring capabilities attainable with Nd:YAG and CO<sub>2</sub> lasers have meant that spot welding is a standard application for these devices [37,38]. However, one of the prime advantages of the Nd:YAG

laser over the CO<sub>2</sub> laser is the ability to deliver laser radiation through optical fibers. This is attractive in robotic or multi-axis laser welding applications. The pulsed Nd:YAG laser welder has been utilized for this study. The pulsed Nd:YAG laser beam has a reputation for rapid, precise and easy operation in welding. However, the use of the technique in inappropriate settings can reduce its effectiveness in welding applications [39]. Many parameters affect the pulsed Nd:YAG laser welding quality, such as pulse peak value, pulse width, pulse frequency, focus position, flow rate of shielding gas and so forth.

The parameters which control laser welding may be classified as primary and secondary variables as shown in Table 2-2. The desired welding parameters are usually determined based on experience or handbook values. However, this does not insure that the selected welding parameters result in optimal or near optimal welding quality characteristics for the particular welding system and environmental conditions. The lithium-ion secondary battery and its micro-weld position are shown in Fig.2-3.

Table 2-2 Parameters for laser welding

Primary	Secondary
Beam power	Pulse parameters
Travel speed	Plasma control
Focus point	Shielding gases
	Beam mode



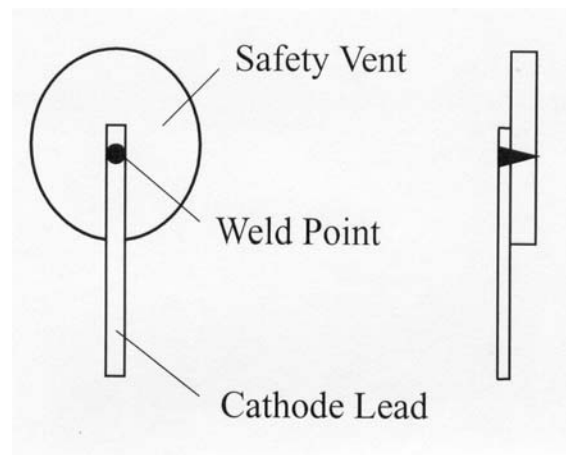
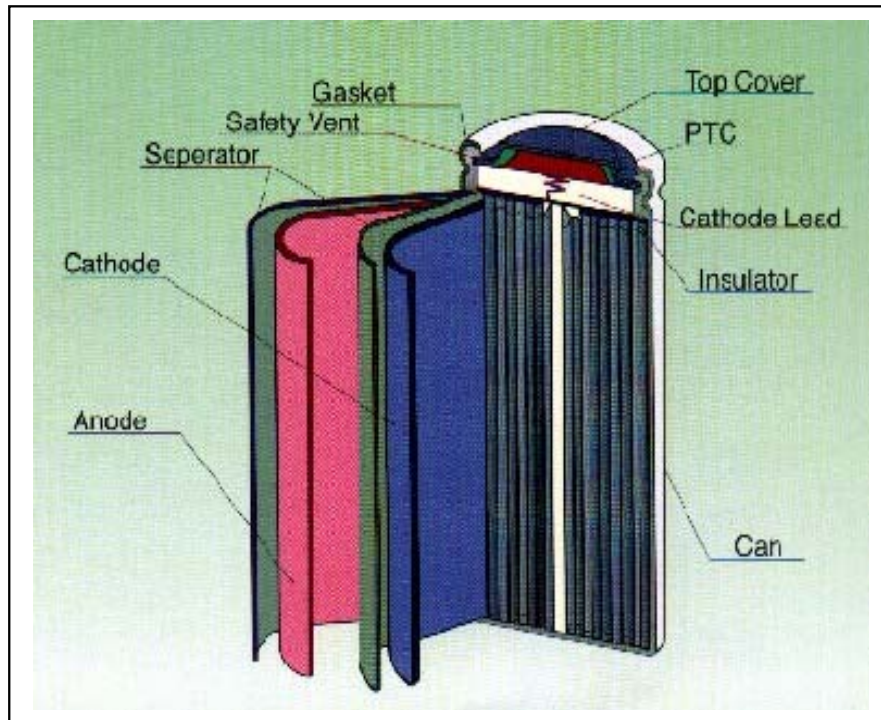
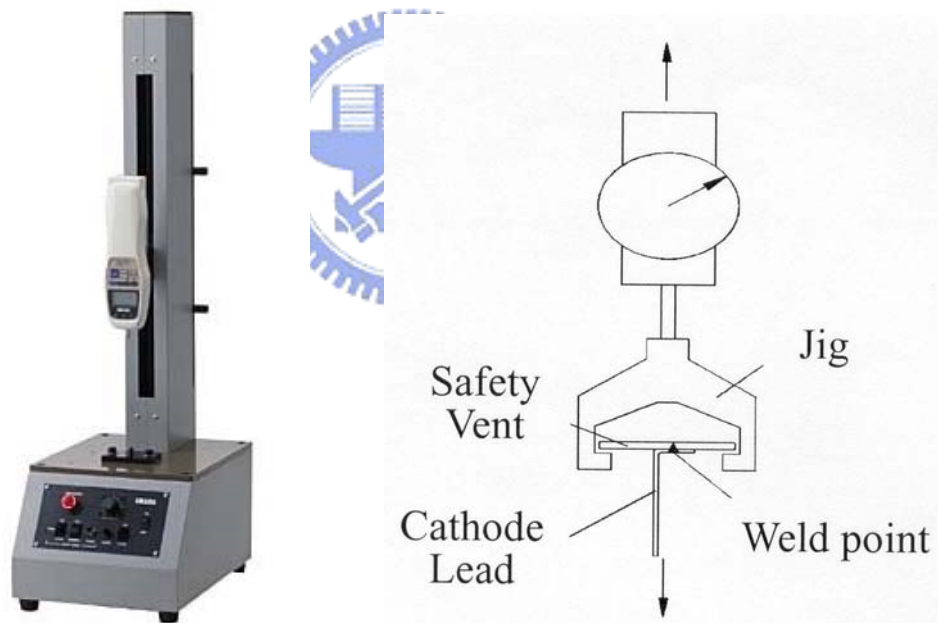


Fig.2-3 Lithium-ion secondary battery and its micro-weld position

### ***Quality characteristic of Nd:YAG laser micro-weld***

Amongst the evaluation frequently used to assess the spot weld characteristic of welding products, the outcome of tensile-shear test on weldment shows more objective for the evaluation of their quality. This study has used the Max. Load of tensile-shear test specimens as the quality characteristic in the process. Tensile force testing instrument (IMADA MV-200BA type) has been used to measure the Max. Load of the laser spot welding specimens. The speed has been set at 6 in  $\text{min}^{-1}$  in the testing process. The measuring way is shown as Fig.2-4.



(IMADA MV-200BA type)

Fig.2-4 Testing instrument and the schematic of measurement

### ***The parameters of the Nd:YAG laser welding***

Fig.2-5 is the cause-effect diagram of the Nd:YAG laser welding process in the mass production process of lithium-ion secondary batteries.

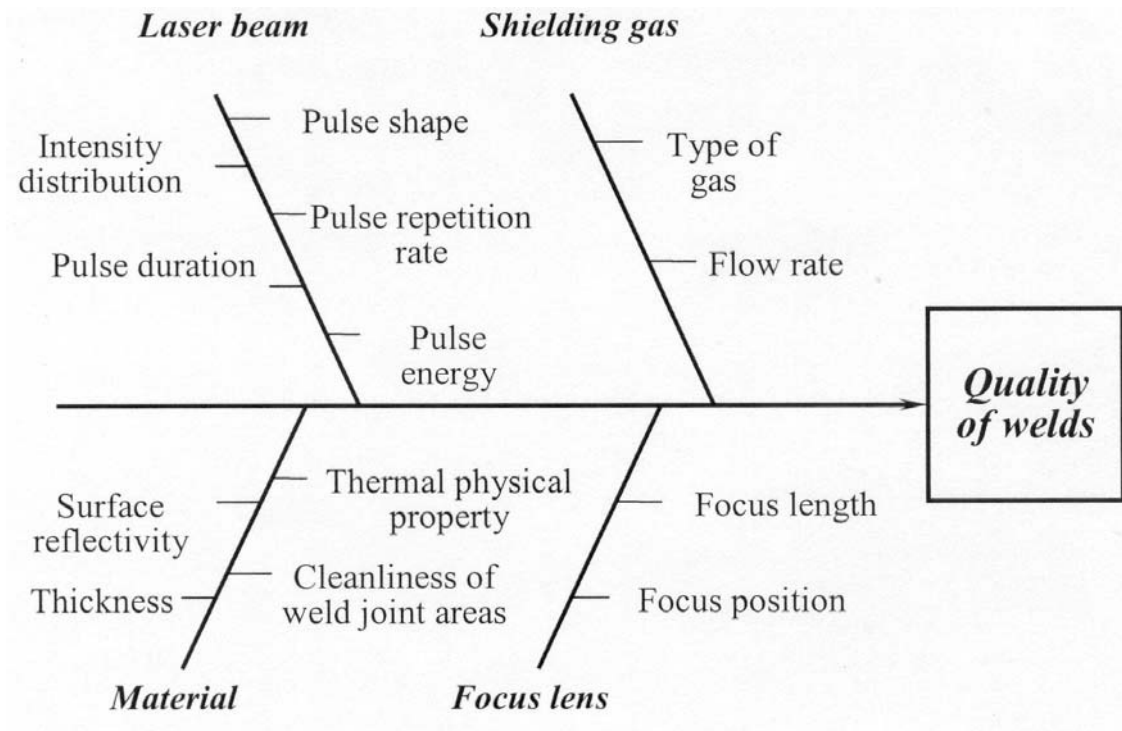


Fig.2-5 Cause and effect diagram of the Nd:YAG laser welding

### **2.6 Resistance spot welding (RSW) in automotive industry**

Resistance welding is widely used by mass production, where production runs and consistent conditions are maintained. RSW is a resistance welding process that produces a weld at the faying surfaces of a joint by the heat obtained from resistance to the flow of welding current through the work pieces

from electrodes that serve to concentrate the welding current and pressure at the weld area [1]. The RSW process is especially used in automobile industry. There has been a significant increase in the use of high strength steel sheet in automobile industry to permit reductions in thickness and thus in vehicle weight [40]. The substitution of high strength steel sheet for thicker plain carbon steels helps to lower weight and meet federally mandated improvements in fuel economy. Resistance welding is widely used in mass production, in which production runs with a consistent condition. The resistance spot welding (RSW) process is especially used in the automobile industry [1]. However, high strength steel sheet has narrow welding current ranges in the RSW process. Sometimes, this limited weldability is a consequence of the interfacial failure of the weld nugget, producing an apparently smaller fusion zone [41]. The physical variables of the metal may include not only the composition of the steels, but also the surface condition. Surface effects have been studied and found to have noticeable effects on spot weldability [42]. In summary, it is not easy to obtain optimal parameters of the RSW process on high strength steel sheet. Many parameters affect the RSW quality for high strength steel sheet, such as welding current, electrode force, welding time and so forth. The desired welding parameters are usually determined based on experience (Try & error) or handbook values (e.g., RWMA). However, it does not insure that the selected welding parameters result in optimal or near optimal welding quality characteristics for the particular welding system and environmental conditions.

### ***Quality characteristic and parameters of RSW process***

The study used Max. Load of tensile-shear test specimens as the quality characteristic in the process. A universal testing machine as shown in Fig.2-6

had been used for this study to measure the Max. Load of the RSW specimens. The speed was set at  $0.1 \text{ mm sec}^{-1}$  in the testing.



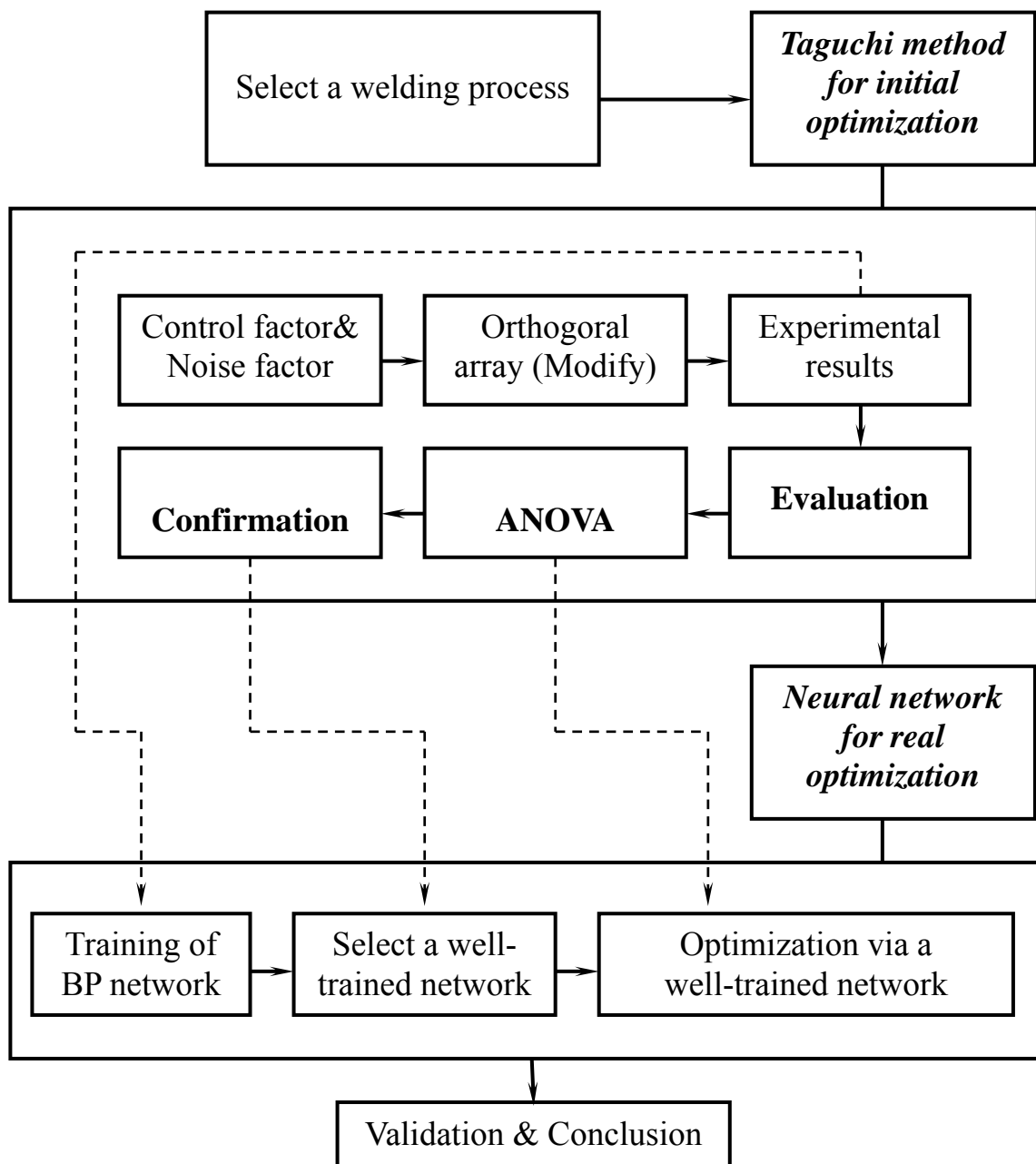
Fig. 2-6 Universal testing machine used

As learned from handbook and the practical experience in the production of auto-body, the major welding parameters for the processing quality of weldment include welding current, welding time, electrode force, the size of electrode tip, and surface condition of specimens in the RSW process.

# CHAPTER 3

## EXPERIMENTAL PROCEDURES

### 3.1 Proposed procedure



In this dissertation, the proposed approach consists of two phases. Phase 1 executes initial optimization via Taguchi method to construct a database for the neural network. Phase 2 applies a neural network with the Levenberg-Marquardt back-propagation (LMBP) algorithm to search for the optimal parameter combination. Three examples involving the gas tungsten arc (GTA) welding, the pulsed Nd:YAG laser micro-weld process, and the resistance spot welding (RSW) process in automotive industry demonstrate the effectiveness of the proposed approach.

## 3.2 Optimization for GTA welding

### 3.2.1 Initial optimization for GTA welding

JIS SUS 304 stainless steel was used in this study with its chemical composition being listed in Table 3-1. The test specimens had the dimensions 50 ×100×2.8 mm. Autogenous (no filler metal was added) and GTA welding was conducted using an EWTh-2 electrode to produce a bead-on-plate weld. A servomechanism controlled the traveling speed of the electrode. The GTA welder (HORBART TIGWAVE™ 350AC/DC type ) has been utilized for the experiment, as shown in Fig.3-1.

Table 3-1 Material used in GTA welding (wt-%)

Material	C	Si	Mn	P	S	Cr	Ni	Fe
JIS SUS 304 Stainless Steel	0.07	0.44	0.95	0.026	0.013	18.7	8.16	Balance





Fig. 3-1 The equipment of Autogenous GTA welder

As shown in Fig.2-1, the  $W$  and  $D$  value of the specimens of type A were measured by a Nonus (Pierre Vernier) with 0.02 mm precision. An optical microscope was used to measure the specimens of Type B. All metallographic specimens were prepared by mechanical lapping, grinding, and polishing to 0.3  $\mu\text{m}$  finish, followed by etching in a solution of 10g.CuSO<sub>4</sub> + 50ml.HCl + 50ml.H<sub>2</sub>O.



### ***Control and noise factor of the GTA welding***

Taguchi separates factors into two main groups, the control factor and noise factor. Control factors are those that allow a manufacturer to control during processing and the noise factors are expensive and difficult to control [10]. Welding current, travel speed of the welding torch, arc length, flow rate of the shielding gas, electrode size and its angle were selected as the controlling factors. The value of each welding process parameter at the different levels is listed in Table 3-2.

Table 3-2 Control factors of GTA welding

Factor	Process parameter	Level 1	Level 2	Level 3
A	Electrode size	$\phi$ 2.4 mm	$\phi$ 3.2 mm	—
B	Electrode angle	70°	75°	80°
C	Arc length	1.0 mm	1.5 mm	2.0 mm
D	Welding current	80 A	85 A	90 A
E	Travel speed	85 mm min <sup>-1</sup>	90 mm min <sup>-1</sup>	95 mm min <sup>-1</sup>
F	Flow rate	8 L min <sup>-1</sup>	10 L min <sup>-1</sup>	12 L min <sup>-1</sup>

The fundamental principle of Robust Design is to improve the quality by minimizing the effect of the causes of variation. It is important in every Robust Design project to identify important noise factors [10]. Engineering experience and judgment are needed in identifying the noise factor. Cleanliness of the weld joint areas was selected as the noise factor in this study. The surface impurities were removed and cleaned with acetone at level one (N1). The specimens at level two (N2) without any cleaning treatment may have been tarnished with dirt and / or grease.

### ***Orthogonal array experiment***

One two-level and five three-level control factors in addition to one noise factor were considered in this investigation. The interaction effect between the welding parameters was not considered. Therefore, there are 11 degrees of freedom owing to the 6 control factors. The degrees of freedom for the OA should be greater than or at least equal to those for the process parameters. The standard arrays available are  $L_{18}$  and  $L_{27}$ .  $L_{18}$  has 8 columns, but provides low resolution. The  $L_{27}$  has 13 columns with greater resolution than  $L_{18}$ .  $L_{27} (3^{13})$  OA was employed in this study.

The “dummy level technique ” was then used for modifying  $L_{27} (3^{13})$  OA into  $L_{27} (2^1 \times 3^5)$  OA. The control factor A was assigned to the column 1 of  $L_{27}$  OA by using dummy levels  $A_3=A_2'$ . Other control factors (B~F) were assigned to the column 2 ~ 6. An experimental layout with an inner array for control factors and an outer array for a two-level noise factor (N1 and N2) is shown in Table 3-3.

There are  $27 \times 2 = 54$  separate test conditions, four repetitions for each trial

are planned in this experimental arrangement. In the Taguchi method, repetitions are used to assess the noise effect on some quality characteristic(s) of interest. Fig.3-2 shows the measuring procedure of weld pool geometry.

Table 3-3 Experimental layout using an  $L_{27}$  orthogonal array

Trial no.	Control factor						Noise factor			
	A	B	C	D	E	F	N1		N2	
							Y <sub>1</sub>	Y <sub>2</sub>	Y <sub>3</sub>	Y <sub>4</sub>
1	1	1	1	1	1	1				
2	1	1	1	1	2	2				
3	1	1	1	1	3	3				
.	.	.	.	.	.	.	<i>Measure data</i>			
.	.	.	.	.	.	.				
26	2	3	2	1	2	1				
27	2	3	2	1	3	2				

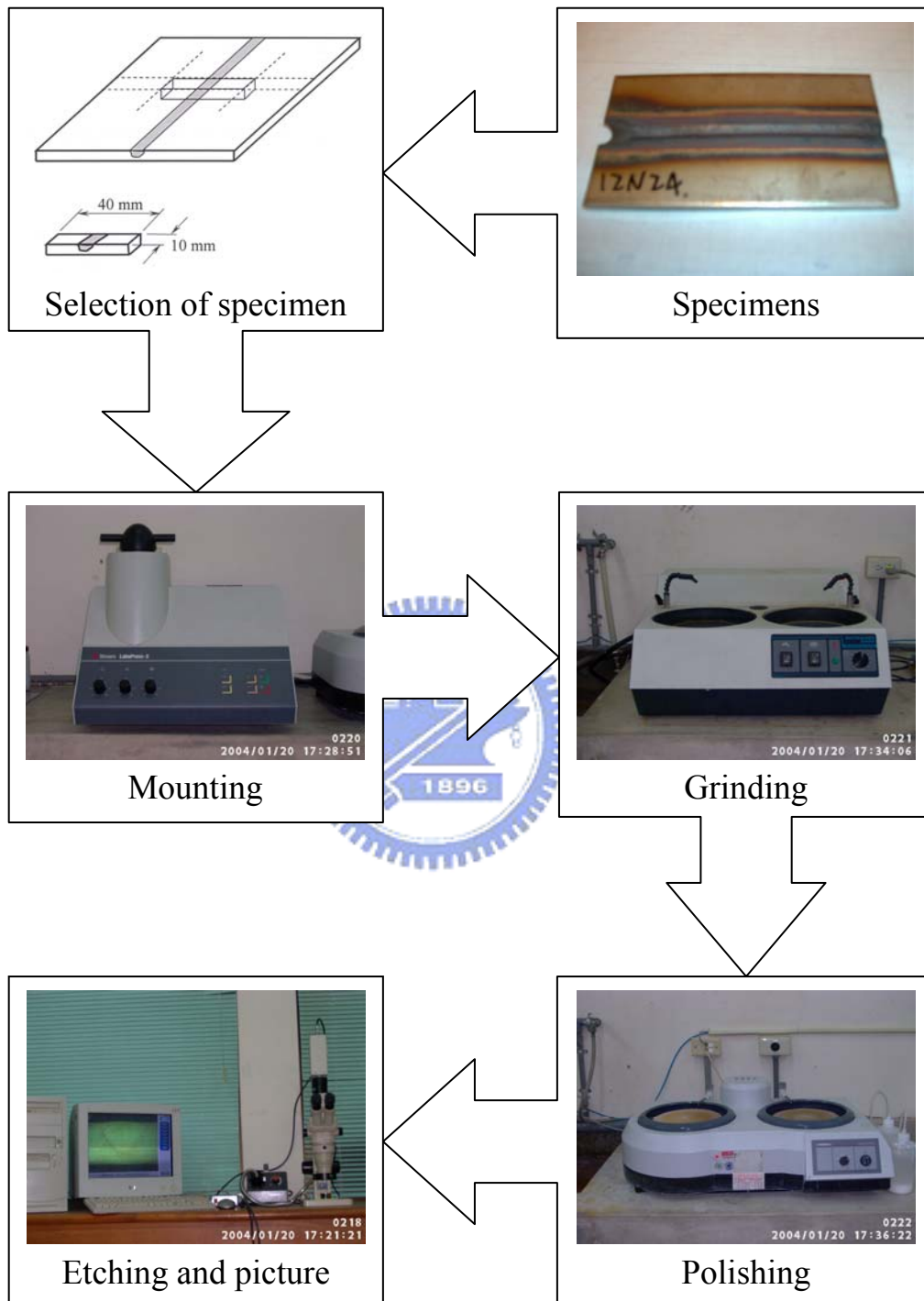


Fig. 3-2 Measurement of weld pool geometry

### ***Evaluation of initial optimal condition***

The depth-to-width ratios (DWR) of the weld pool geometry as discussed earlier belong to the higher-is-better quality characteristic. The  $S/N$  ratios, which condense the multiple data points within a trial, depend on the type of characteristic being evaluated. The equation for calculating  $S/N$  ratio for HB characteristic is

$$S / N = -10 \log_{10} \left( \frac{1}{n} \sum_{i=1}^n \frac{1}{y_i^2} \right) \quad 3-1$$

where  $n$  is the number of tests in a trial (number of repetitions regardless of noise levels). The value of  $n$  is 4 in this study. The  $S/N$  ratio corresponding to the  $D/W$  ratio of each trial is shown in Table 3-4. The effect of each welding process parameter on the  $S/N$  ratio at different levels can be separated out because the experimental design is orthogonal. The description of the  $S/N$  ratio for each level of the welding process parameters is summarized and shown in Table 3-5.

Table 3-4 Summary of experiment data of GTA welding

Trial no.	Control factors						Depth-to-width ratio	
	A	B	C	D	E	F	Average	S/N ratio, dB
1	1	1	1	1	1	1	0.624	-4.10
2	1	1	1	1	2	2	0.482	-6.34
3	1	1	1	1	3	3	0.392	-8.15
4	1	2	2	2	1	1	0.697	-3.14
5	1	2	2	2	2	2	0.694	-3.17
6	1	2	2	2	3	3	0.604	-4.38
7	1	3	3	3	1	1	0.608	-4.33
8	1	3	3	3	2	2	0.605	-4.37
9	1	3	3	3	3	3	0.407	-7.81
10	2	1	2	3	1	2	0.685	-3.29
11	2	1	2	3	2	3	0.667	-3.52
12	2	1	2	3	3	1	0.661	-3.59
13	2	2	3	1	1	2	0.670	-3.48
14	2	2	3	1	2	3	0.638	-3.91
15	2	2	3	1	3	1	0.641	-3.86
16	2	3	1	2	1	2	0.664	-3.56
17	2	3	1	2	2	3	0.675	-3.41
18	2	3	1	2	3	1	0.569	-4.91
19	2	1	3	2	1	3	0.672	-3.45
20	2	1	3	2	2	1	0.696	-3.14
21	2	1	3	2	3	2	0.564	-4.98
22	2	2	1	3	1	3	0.702	-3.08
23	2	2	1	3	2	1	0.696	-3.15
24	2	2	1	3	3	2	0.688	-3.51
25	2	3	2	1	1	3	0.488	-6.23
26	2	3	2	1	2	1	0.511	-5.83
27	2	3	2	1	3	2	0.343	-9.31

Table 3-5 *S/N* response table for the weld pool geometry

Factor	Process parameter	Level 1	Level 2	Level 3
A	Electrode size	- 5.088	- 4.234	—
B	Electrode angle	- 4.508	- 3.520	- 5.529
C	Arc length	- 4.467	- 4.719	- 4.370
D	Welding current	- 5.691	- 3.794	- 4.072
E	Travel speed	- 3.851	- 4.095	- 5.611
F	Flow rate	- 4.006	- 4.669	- 4.882

Fig.3-3 shows the *S/N* ratio graph that the data obtained from Table 3-5. Basically, the larger is the *S/N* ratio, the better the quality characteristic (depth-to-width ratio) is for the weld pool geometry. The initial optimal combinations of the GTA welding process parameter levels,  $A_2B_2C_3D_2E_1F_1$ , can be determined by means of Fig. 3-3.

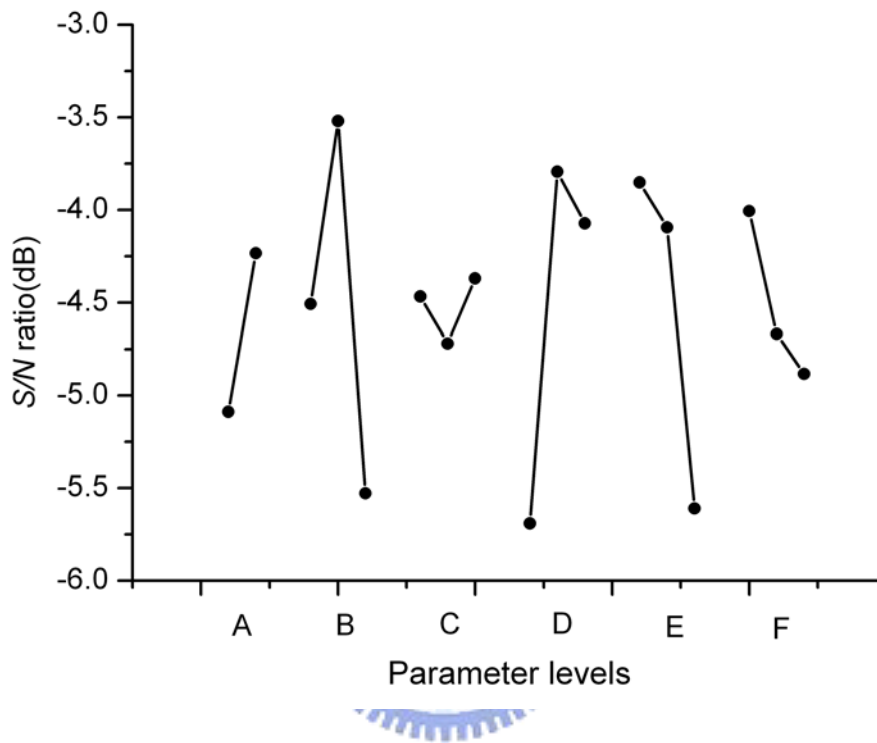


Fig. 3-3 S/N graph for the weld pool geometry

### *Analysis of variance*

The electrode angle, welding current, travel speed, and arc length were the significant welding parameters in affecting the quality characteristic, with the welding current and electrode angle being the most significant, as indicated from Table 3-6.



Table 3-6 Results of ANOVA for the weld pool geometry

Factor	Process parameter	Degree of freedom	Sum of square	Mean square	F- Test	Pure sum of square	Percent contribution
A	Electrode size	1	4.369	4.369	5.66	3.60	4.82%
B	Electrode angle	2	18.165	9.082	11.77	16.62	22.26%
C	Arc length	2	0.584 *				
D	Welding current	2	18.892	9.4463	12.24	17.35	23.23%
E	Travel speed	2	16.355	8.178	10.59	14.81	19.84%
F	Flow rate	2	3.760	1.880	2.44	2.22	2.97%
Error		15	12.540				
Error (pooled)		(17)	(13.123)	(0.772)		20.07	26.88%
Total		26	74.66			74.66	100%

Mark \*means the factors are treated as pooled error

**Confirmation tests**

An interval confidence of 95% for the depth-to-width ratio, the  $F_{0.05;1;17}$  =4.45,  $v_{ep}$  =0.772, the sample size for the confirmation experiment  $r$  is 2,  $N$  =27,  $DOF_{opt}$  =6, and the effective sample size is  $n_{eff}$  =3.857. Thus, the

confidence interval is computed as  $CI = 1.62(\text{dB})$ . The experimental results (Table 3-7) confirm that the initial optimizations of the GTA welding process parameters were achieved.

Table 3-7 Confirmation experiment of GTA welding

Trial no.	Depth-to-width ratio				Confidence interval (95%)		
	N1 specimens		N2 specimens			Average	
28	0.696	0.712	0.676	0.683	-3.302	0.691	-2.12 ±
29	0.683	0.701	0.682	0.696	-3.219	$\left( \begin{array}{l} D = 3.346\text{mm} \\ W = 4.843\text{mm} \end{array} \right)$	1.62 (dB)

### 3.2.2 Real optimization for GTA welding

#### *Training of BP network*

A feed-forward neural network is proposed for this study. It takes a set of six input values (control factors A, B, C, D, E, and F) and predicts the value of two outputs ( $D$  and  $W$  value of the weld pool geometry). A total of 108 input-output data patterns were partitioned into a training set and a testing set. Functionally, 80% (approximately 87 patterns) were randomly selected for training the neural network while the remaining 20% (approximately 21 patterns) were used for testing. An efficient algorithm, the Levenberg-Marquardt

algorithm, was used to improve classical back-propagation learning in the training process. Table 3-8 presents eight options of the neural network architecture. Under the less simulating error that compared with average value of  $W$  and  $D$  in Table 7 and best convergence criterion of the mean square error (MSE) of the testing subset, the structure 6-7-2 was selected to obtain a better performance. The topology of the network 6-7-2 with a  $0.001 \mu$  value and a  $\theta$  value of 10 is depicted in Fig.3-4.

Table 3-8 Options for different networks in GTA welding

Architecture (Input-hidden unit-output)	MSE for training	Simulating error, % (Compare with average value in Table 3-7)	
		$W$ value	$D$ value
6-2-2	0.057447	- 4.65	0.29
6-3-2	0.043527	2.01	5.82
6-4-2	0.043214	- 5.28	1.36
6-5-2	0.073604	0.53	8.54
6-6-2	0.023242	- 59.32	- 21.84
6-7-2	0.041730	- 1.44	5.28
6-8-2	0.044620	- 8.34	0.36
6-9-2	0.011117	36.05	13.15

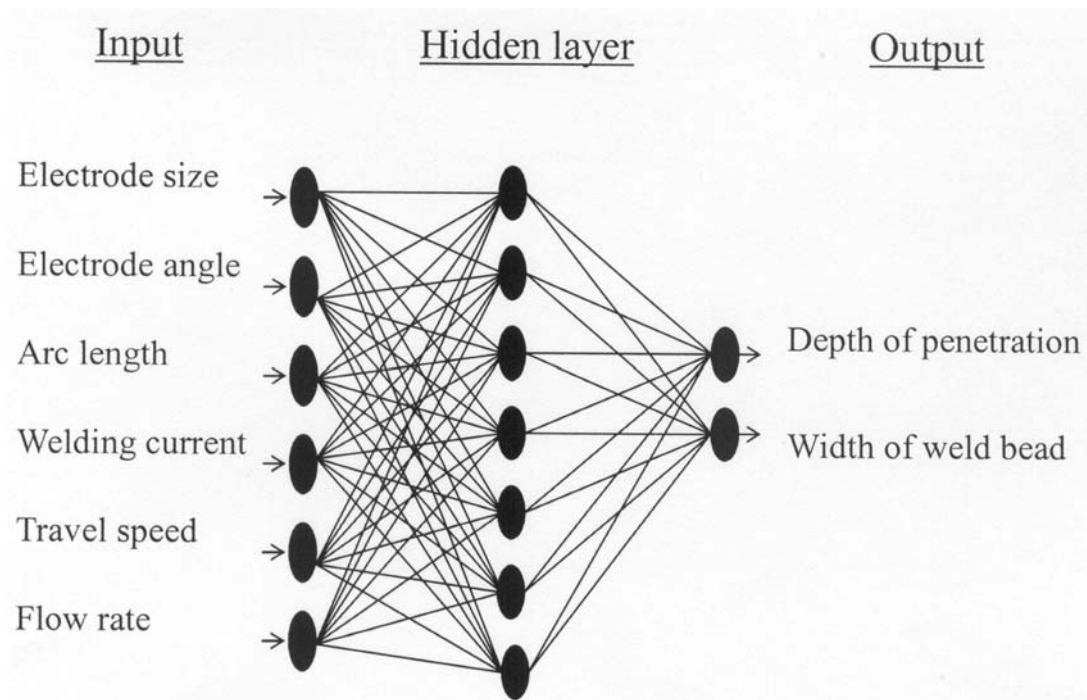
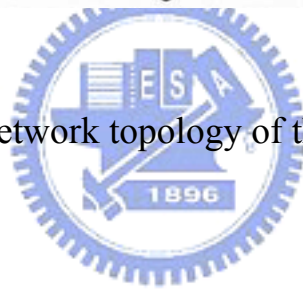


Fig. 3-4 The BP network topology of the GTA welding process



### ***Optimization with trained network***

The control factor B (electrode angle) and D (welding current) are the significant welding parameters in affecting the quality characteristic (depth-to-width ratio of each weldment) as shown in Table 3-6. The trained network 6-7-2 was employed as the simulating function of the primary parameters in this welding process. Fig.3-5 shows the comparison of simulating results using the significant welding parameters (factor B and D) obtained by the Taguchi method, from which it can be seen that the depth-to-width ratio of weld pool geometry is best for adjusting welding current to 81 A and electrode to 73 degree of angle.

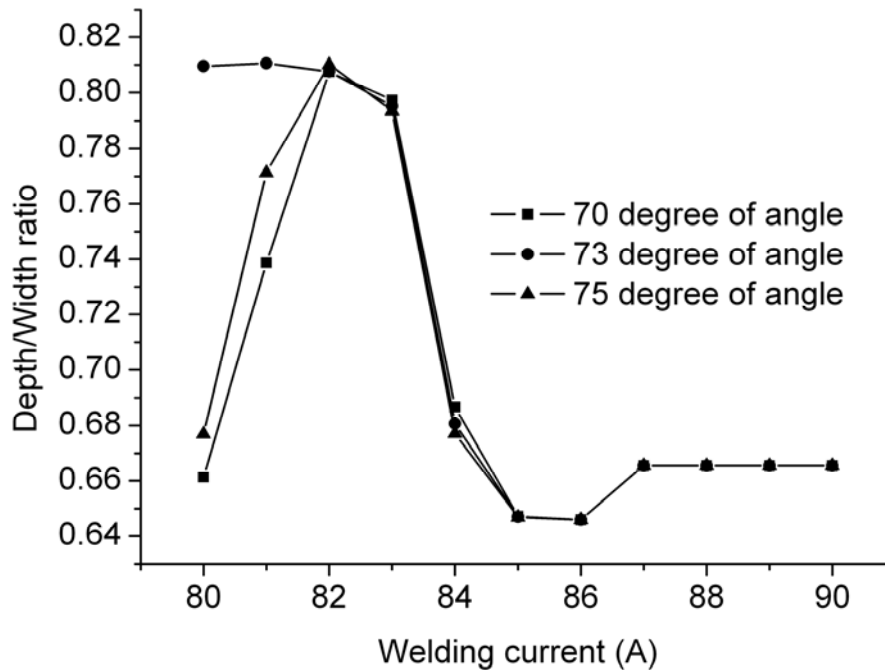
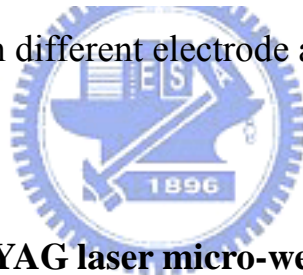


Fig. 3-5 Simulation different electrode angle and welding current



### 3.3 Optimization for Nd:YAG laser micro-weld

#### 3.3.1 Initial optimization for Nd:YAG laser micro-weld

The materials of safety vent and cathode lead used for lithium-ion secondary batteries are AA3003 aluminum alloy (Please refer to Table 3-9 for its chemical composition). The safety vent had the dimensions  $\phi 18 \times 1.0$  mm; cathode lead had the dimensions  $3 \times 70 \times 0.1$  mm. The pulsed Nd:YAG laser spot welder (Toshiba Lay-822H type) has been utilized for the experiment. The wavelength of laser is  $1.06 \mu\text{m}$  and through the fiber conduction, the laser beam is to joint the product, as shown in Fig.3-6. Fig.3-7 shows the illustration of automatic mass production for the lithium-ion secondary battery parts (safety vent and cathode lead).

Table 3-9 Material used in Nd:YAG laser spot welding (wt-%)

Material	Si	Cu	Mn	Zn	Others	Al
AA3003 Aluminum Alloy	0.7	0.05~0.2	1.0~1.5	0.1	0.15	Balance



Fig.3-6 Pulsed Nd:YAG laser spot welder



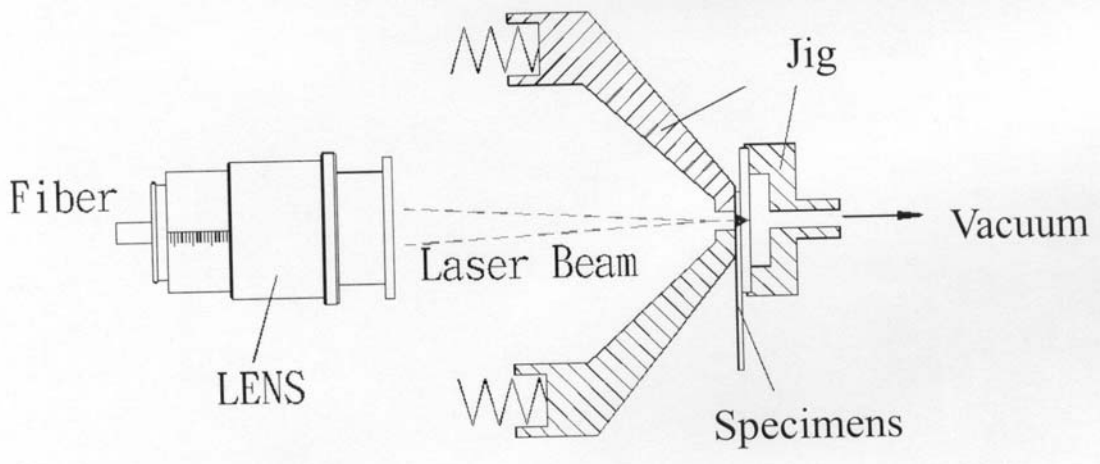
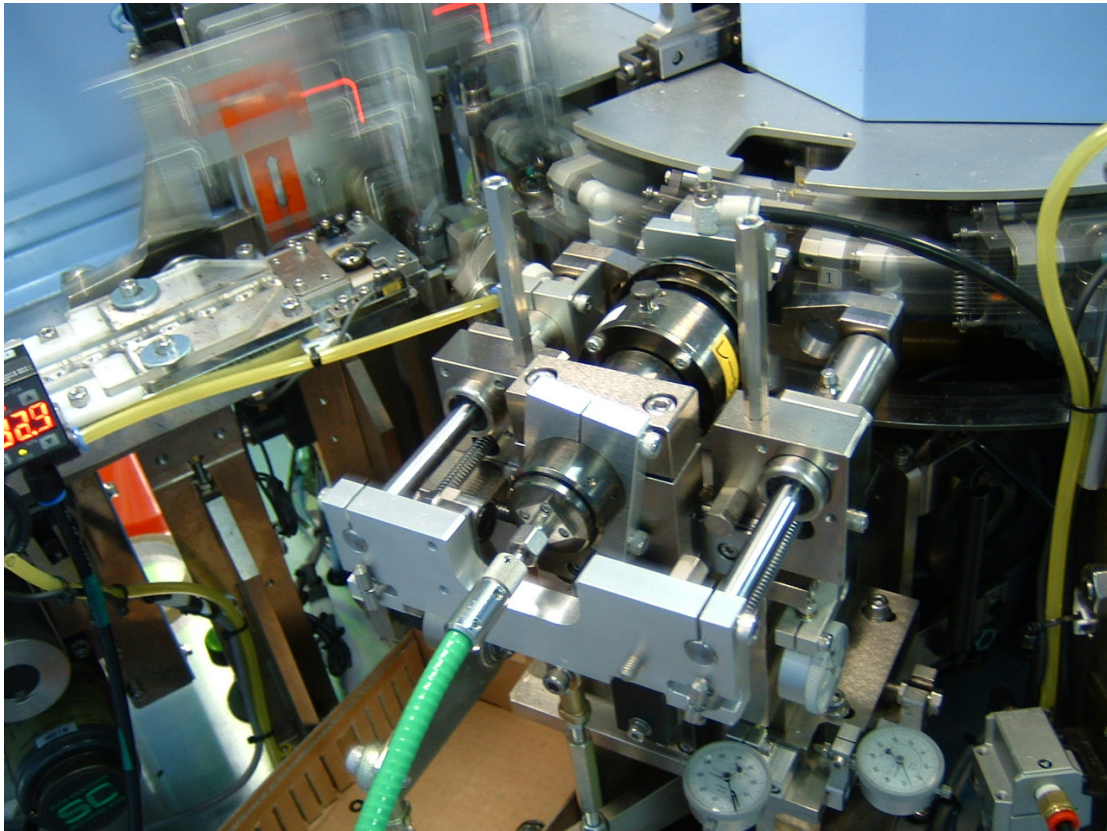


Fig.3-7 Illustration of automatic production

The Max. Load of weldment lower than 0.5 kg were determined to defective products, as suggested by the engineers of a manufacturing lithium-ion secondary batteries company in Taiwan. To prevent leakage from “safety vent”, Max. Load was restricted under 1.2 kg. In practice, the higher energy of pulsed Nd:YAG laser welding (e.g., higher pulse peak value), the deeper penetration of weldment being obtained. The deeper penetration of weldment (between “safety vent” and “cathode lead”) would be increasing the Max. Load. However, it may be pierce through the “safety vent” and result in leakage of lithium-ion secondary batteries in the future. Summary, increasing Max. Load of weldment to 1.0 kg and decreasing the defective rate under 5% is attempted in this study.

### ***Control and noise factor of Nd:YAG laser micro-weld***

As learned from the literature [43] and the experience in the production process of lithium-ion secondary batteries, the major welding parameters for the pulsed Nd:YAG laser spot welding quality of weldment include pulse peak value, pulse width, pulse frequency and focus position. The parameters as mentioned above may be respectively adjusted within the range as below: pulse peak value 0 ~ 500 Volt, pulse width 0.2 ~ 20.0 msec, pulse frequency 0.5 ~ 20 pps and focus position -1.0 ~ +1.0 mm. The values of the welding process parameters at the different levels are listed in Table 3-10.

Aluminum and its alloys have high reflectivity together with large thermal conductivity; it is a poor absorber of laser light. Laser welding of aluminum and its alloys is difficult and the weld quality is often very poor [37,38]. Another problem that adversely affects welding of aluminum and its alloys is the natural oxide and other contamination on the material surface. So, the cleaning



treatment on “safety vent” and “cathode lead” of lithium-ion secondary batteries (AA3003 aluminum alloy) surface is very important. Unfortunately, it is very hard to control the surface cleanliness of the weldment in the automatic mass production. Thus, cleanliness of the weld joint areas was selected as the noise factor of Taguchi method in this study. The surface impurities were removed and the surface was cleaned with acetone at level one (N1, 100% cleanliness). The specimens at level two (N2, 0% cleanliness), without any cleaning treatment, may have been tarnished with dirt and / or grease.

Table 3-10 Control factors of Nd:YAG laser spot welding

Factor	Process parameter	Level 1	Level 2	Level 3	Level 4	Level 5
A	Focus position (mm)	- 0.5	0	+ 0.5	—	—
B	Pulse peak value (Volt.)	300	315	330	345	360
C	Pulse width (msec)	4	5	6	7	8
D	Pulse frequency (pps)	1	1.5	2	2.5	3

### ***Orthogonal array experiment***

One two-level and three five-level control factors, in addition to one noise factor, were considered in this investigation. The interaction effect between the welding parameters was not considered. Therefore, there are 14 degrees of freedom, owing to the four control factors. The degrees of freedom for the OA should be greater than or at least equal to those for the process parameters. The  $L_{25} (5^6)$  OA was employed in this study. The ‘dummy level technique’ was then used for changing the  $L_{25} (5^6)$  OA into the  $L_{25} (3^1 \times 5^3)$  OA. Control factor A was assigned to the column 1 of  $L_{25}$  OA by using dummy levels  $A_2=A_1'$ ,  $A_3=A_2'$ ,  $A_4=A_3'$  and  $A_5=A_3'$ . Other control factors (B~D) were assigned to the column 2 ~ 4. Note that the orthogonality was preserved even when the dummy level technique was applied to one or more factors.

In addition, the noise factor could be assigned to the outer array to determine some level of a control factor that does not give much variation in the results, even though a noise factor is definitely present. An experimental layout with an inner array for control factors and an outer array for a two-level noise factor (N1 and N2) is shown in Table 3-11. There are  $25 \times 2 = 50$  separate test conditions; four repetitions for each trial ( $y_1$ ,  $y_2$ ,  $y_3$  and  $y_4$ ) were planned in this experimental arrangement;  $y_1$  and  $y_2$  are N1 specimens (cleaned with acetone),  $y_3$  and  $y_4$  are N2 specimens (without cleaning). In the Taguchi method, repetitions are used to assess the noise effect on some quality characteristic(s) of interest.

Table 3-11 Experimental layout using  $L_{25}$  orthogonal array

Trial no.	Control factor				Noise factor			
	A	B	C	D	N1 specimens		N2 specimens	
					y <sub>1</sub>	y <sub>2</sub>	y <sub>3</sub>	y <sub>4</sub>
1	1	1	1	1				
2	1	2	2	2				
3	1	3	3	3				
4	1	4	4	4				
5	1	5	5	5				
6	1	1	2	3				
7	1	2	3	4				
8	1	3	4	5				
9	1	4	5	1				
10	1	5	1	2				
11	2	1	3	5				
12	2	2	4	1				
13	2	3	5	2				
14	2	4	1	3				
15	2	5	2	4				
16	3	1	4	2				
17	3	2	5	3				
18	3	3	1	4				
19	3	4	2	5				
20	3	5	3	1				
21	3	1	5	4				
22	3	2	1	5				
23	3	3	2	1				
24	3	4	3	2				
25	3	5	4	3				

Measure data

### ***Evaluation of initial optimal condition***

The tensile-shear strength of the specimens, as discussed earlier, belongs to the HB quality characteristic. The SNRs, which condense the multiple data points within a trial, depend on the type of characteristic being evaluated. The equation for calculating the SNR ratio for HB characteristic is

$$SNR = -10 \log \left( \frac{1}{n} \sum_{i=1}^n \frac{1}{y_i^2} \right) \quad 3-2$$

where  $n$  is the number of tests in a trial (number of repetitions regardless of noise levels) and  $y_i$  is the Max. Load of each specimens. The value of  $n$  is 4 in this study. The SNR corresponding to Max. Load of each trial is shown in Table 3-12. The effect of each welding process parameter on the SNR at different levels can be separated out because the experimental design is orthogonal. The description of the SNR for each level of the welding process is summarized in Table 3-13. Fig.3-8 shows the SNR graph obtained from Table 3-13. Basically, the larger the SNR, the better the quality characteristic (tensile-shear strength) is for the specimens. The initial optimal combinations of the pulsed Nd:YAG laser micro-weld process parameter levels,  $A_3B_5C_3D_5$ , can be determined from Fig.3-9.

Table 3-12 Experiment data of Nd:YAG laser micro-weld

Trial no.	Max. Load, kg				Average	SNR, dB
	y <sub>1</sub>	y <sub>2</sub>	y <sub>3</sub>	y <sub>4</sub>		
1	0.05	0.10	0.01	0.01	0.04	-37.10
2	0.20	0.25	0.10	0.15	0.18	-16.66
3	0.70	0.64	0.50	0.40	0.56	-5.66
4	0.75	0.80	0.65	0.70	0.73	-2.87
5	0.85	1.00	0.80	0.75	0.85	-1.56
6	0.20	0.20	0.15	0.10	0.16	-16.87
7	0.35	0.55	0.30	0.45	0.41	-8.38
8	0.70	0.80	0.50	0.65	0.66	-3.97
9	0.40	0.25	0.35	0.20	0.30	-11.42
10	0.35	0.40	0.45	0.30	0.38	-8.82
11	0.25	0.20	0.20	0.15	0.20	-14.41
12	0.20	0.35	0.20	0.30	0.26	-12.39
13	0.15	0.20	0.15	0.10	0.15	-17.28
14	0.65	0.50	0.35	0.50	0.50	-6.66
15	0.50	0.65	0.40	0.60	0.54	-5.85
16	0.25	0.05	0.15	0.10	0.14	-21.46
17	0.30	0.35	0.40	0.20	0.31	-11.01
18	1.00	0.90	0.60	0.40	0.73	-4.50
19	0.60	0.70	0.50	0.65	0.61	-4.47
20	0.85	0.90	0.70	0.90	0.84	-1.68
21	0.35	0.30	0.10	0.20	0.24	-15.57
22	0.45	0.40	0.30	0.50	0.41	-8.18
23	0.55	0.50	0.35	0.50	0.48	-6.87
24	0.80	0.70	0.60	0.75	0.71	-3.10
25	0.80	0.95	0.70	0.85	0.83	-1.83

Total average of SNR for all trial is -9.942 (dB)

Table 3-13 SNR response table for the quality characteristic

Factor	Process parameter	Level 1	Level 2	Level 3	Level 4	Level 5
A	Focus position	-11.329	-11.318	-7.867	-	-
B	Pulse peak value	-21.082	-11.323	-7.656	-5.701	-3.948
C	Pulse width	-13.049	-10.144	-6.646	-8.503	-11.368
D	Pulse frequency	-13.891	-13.464	-8.406	-7.433	-6.516

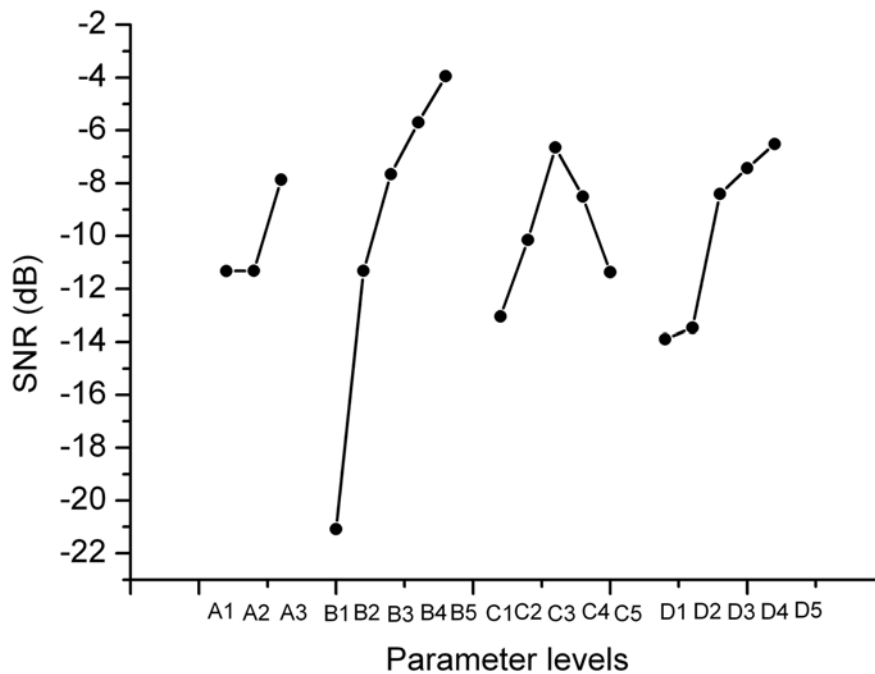


Fig.3-8 SNR graph for the quality characteristic

### *Analysis of variance*

The pulse peak value, pulse frequency and focus position were the significant welding parameters affecting the quality characteristic (tensile-shear strength of each specimen), with the pulse peak value being the most significant, as indicated by Table 3-14.

Table 3-14 Results of ANOVA for the quality characteristic

Factor	Process parameter	Degree of freedom	Sum of square	Mean square	F- test	Pure sum of square	Percent contribution
A	Focus position	2	196.049	98.025	19.75	186.12	12.11%
B	Pulse peak value	4	925.757	231.439	46.63	905.90	58.95%
C	Pulse width	4	123.328	30.832	6.21	103.47	6.73%
D	Pulse frequency	4	241.943	60.486	12.19	222.09	14.45%
Error		10	49.636	4.964		119.13	7.75%
Total		24	1536.71			1536.71	100%

**Confirmation tests for initial optimization**

Refer to Table 3-13 and 3-14, the factor C shows the least effect for quality characteristic. In order to prevent over-estimate [8], factor C is not considered, the estimated SNR  $\eta_{opt}$  is computed as

$$\eta_{opt} = -9.942 + (-7.867 + 9.942) + (-3.948 + 9.942) + (-6.516 + 9.942) = 1.553 \text{ (dB)}$$

With *CI* of 95% for the tensile-shear strength, the  $F_{0.05,1,10} = 4.96$  and  $V_{ep} = 4.964$ , the sample size for the confirmation experiment  $r$  is 3,  $N = 25$ ,  $DOF_{opt} = 10$ , and the effective sample size  $n_{eff}$  is 2.273. Thus, the *CI* is computed to be  $CI = 4.364$  (dB). The experimental results (Table 3-15) confirm that the initial optimizations of the Nd:YAG laser micro-weld process parameters were achieved.



Table 3-15 Confirmation experiment of Nd:YAG laser micro-weld

Trial no.	Max. Load				SNR, dB	Average, kg	Confidence interval, 95%
	N1 specimens	N2 specimens					
26	0.96	1.05	0.83	0.92	-0.63		
27	1.05	1.00	0.90	0.83	-0.60	0.933 N1=1.008 N2=0.858	1.553 ± 4.364 (dB)
28	1.02	0.97	0.82	0.85	-0.88		



### 3.3.2 Real optimization for Nd:YAG micro-weld

#### *Training of BP network*

A feed-forward neural network is proposed for this study. It takes a set of five input values (control factors A, B, C, D and noise factor) and predicts the value of one output (Max. Load of the specimens). A total of 100 input-output data patterns were partitioned into a training set, a testing set and a validating set. Functionally, 60% (60 patterns) were randomly selected for training the neural network the remaining 20% (20 patterns) were randomly used for testing and 20% (20 patterns) were randomly used for validating. An efficient algorithm, the Levenberg-Marquardt algorithm, was used to improve classical BP learning in the training process [17,21]. The neural network package software MATLAB Neural Network ToolBox was used to develop the required network.

Table 3-16 presents fifteen options for the neural network architecture. After comparing all the data for the mean square error (MSE), the structure 5-3-1, 5-15-1, 5-25-1, 5-35-1 and 5-40-1 are the five best convergence criteria. The structure 5-15-1 showed the least error and was therefore selected to obtain a better performance. The topology of the network 5-15-1 with a  $\mu$  value 0.001 and a  $\theta$  value of 10 is shown in Fig. 3-9.

Table 3-16 Options for different networks in Nd:YAG laser welding

Architecture (input-hidden unit-output)	Mean square error for training	Simulating error, % (Compare with average value in Table 3-15)	
		N1 value	N2 value
5-2-1	0.0077	-20.6	-16.6
5-3-1*	0.0046	-26.2	-19.1
5-4-1	0.0121	-14.1	-8.2
5-5-1	0.0052	-21.3	-21.4
5-6-1	0.0078	-21.9	-10.5
5-7-1	0.0304	-25.0	-37.9
5-8-1	0.0119	-31.6	-29.7
5-9-1	0.0064	-24.5	-24.3
5-10-1	0.0083	-16.0	-22.6
5-15-1*	0.0027	5.1	-13.1
5-20-1	0.0099	-33.2	-19.0
5-25-1*	0.0027	-33.7	-62.2
5-30-1	0.0243	-50.9	83.2
5-35-1*	0.0034	-22.9	-33.4
5-40-1*	0.0020	-20.8	-50.6

\*The structures are the five best convergence criteria

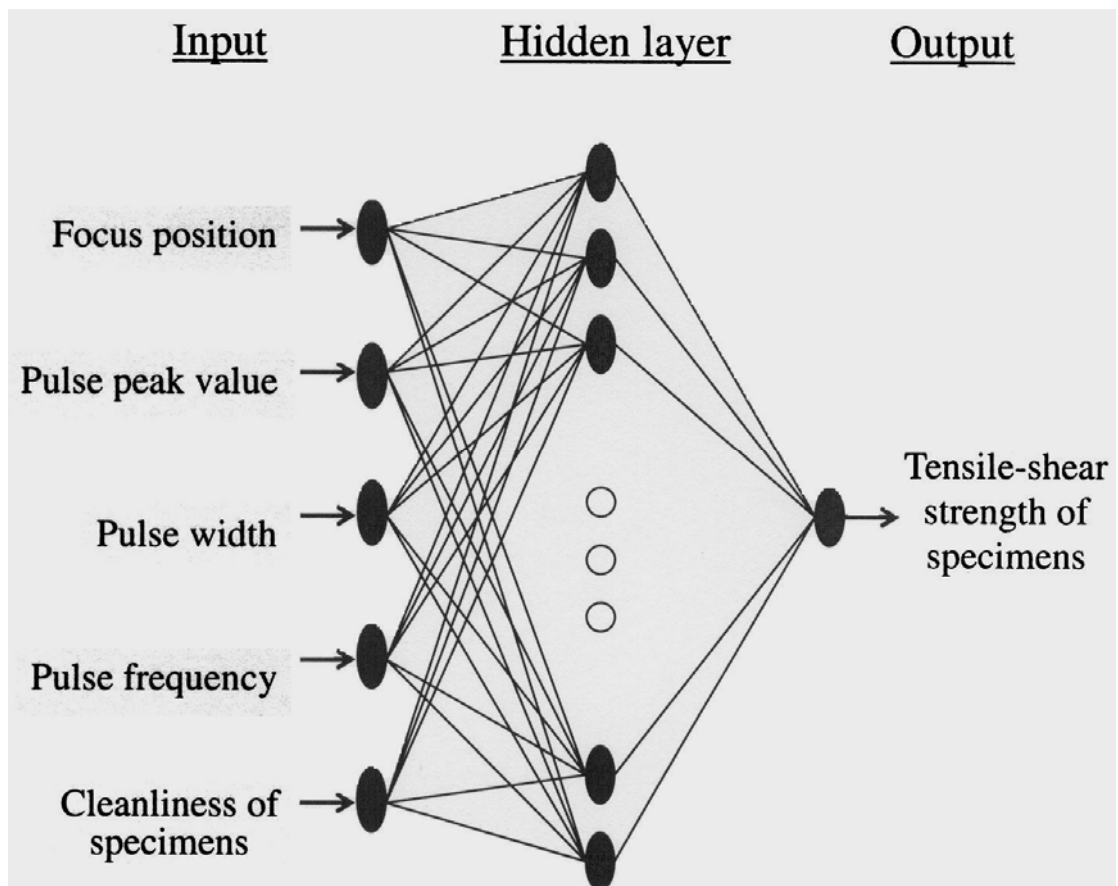


Fig. 3-9 The BP network topology of the Nd:YAG laser welding

### *Optimization with a well-trained network*

The control factor C (pulse width) is the insignificant welding parameters that affect the quality characteristic (Max. load of each specimen) as shown in Table 3-14. First, the trained network 5-15-1 was employed as the simulating function of the control factor C.

Fig.3-10 shows the comparison of simulated results using the pulse width, other conditions  $A_{+0.5\text{mm}}B_{360\text{Volt}}D_{3\text{pps}}$ , from which it can be seen that the tensile-shear strength of specimens is the best ones for setting pulse width to 6 msec.

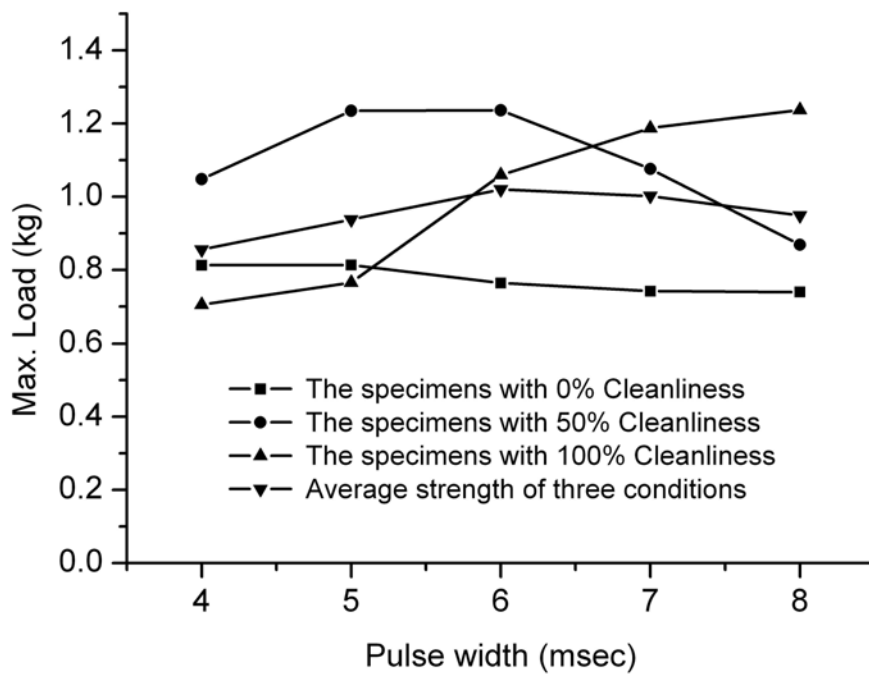


Fig. 3-10 Results of simulating different pulse width

Second, Fig.3-11 shows the comparison of simulated results using the factor A, other conditions  $B_{360\text{Volt}}C_{6\text{msec}}D_{3\text{pps}}$ , from which it can be seen that the tensile-shear strength of specimens is the best ones for adjusting focus position from +0.5 to +0.25 mm.

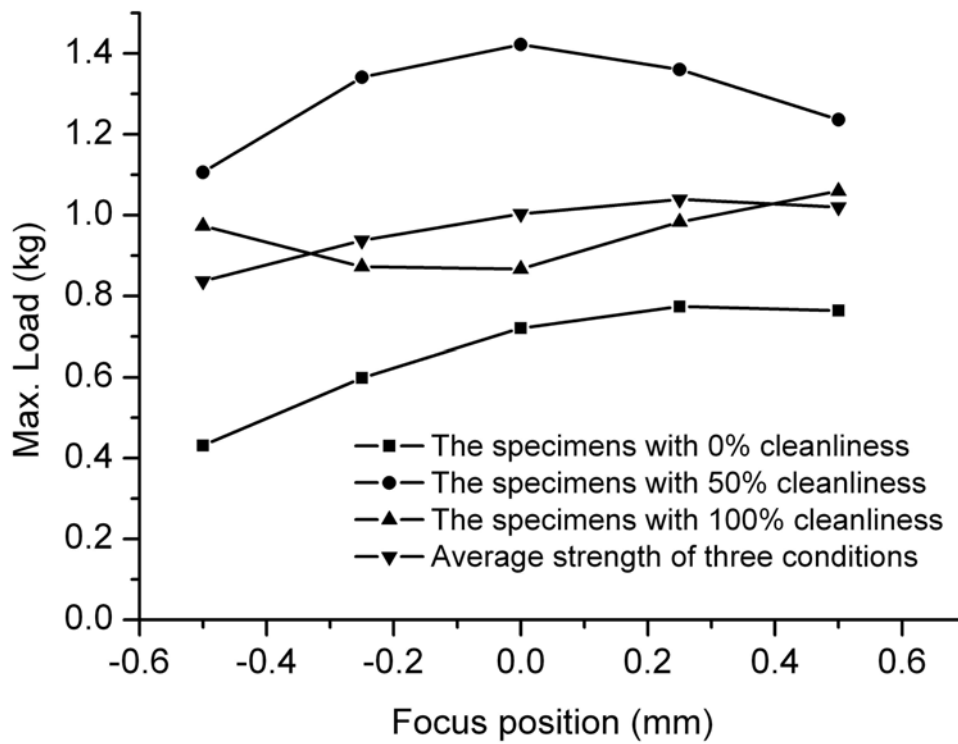


Fig. 3-11 Results of simulating different focus position

Third, Fig.3-12 shows the comparison of simulated results using the factor D, other conditions  $A_{+0.25\text{mm}}B_{360\text{Volt}}C_{6\text{msec}}$ , from which it can be seen that the pulse frequency and Max. Load are in direct ratio. When the pulse frequency is over 2.0 pps, the Max. Load will decrease progressively for N1 specimens (with 100% cleanliness). On the other hand, the Max. Load increased progressively for N2 specimens (with 0% cleanliness). In this study, the pulse frequency was selected on 3.4 pps.

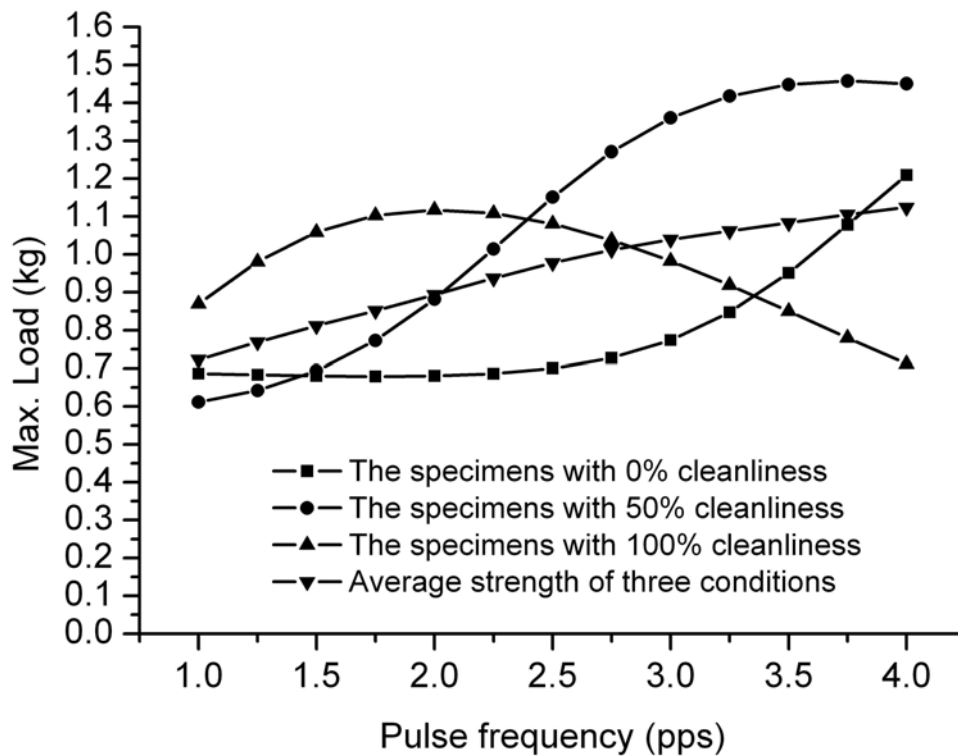


Fig.3-12 Results of simulating different pulse frequency

Finally, Fig.3-13 shows the comparison of simulating results using the factor B, other conditions  $A_{+0.25\text{mm}}C_{6\text{msec}}D_{3.4\text{pps}}$ , from which it can be seen that the pulse peak value and Max. Load are in direct ratio. When the pulse peak value is adjusted over 355 Volt, the tensile-shear strength of specimens will derive to 1.0 kg. In addition, Fig.3-20 shows that the specimens with 50% cleanliness are better than N1 (with 100% cleanliness) and N2 (with 0% cleanliness) specimens.

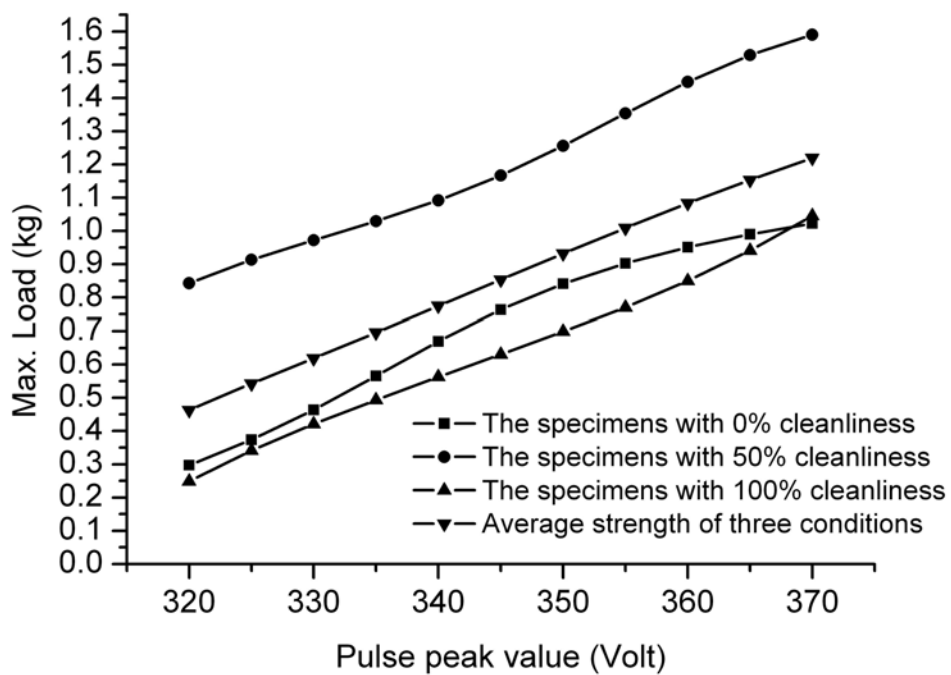


Fig.3-13 Results of simulating different pulse peak value

### 3.4 Optimization for RSW process

#### 3.4.1 Initial optimization for RSW process

The high strength steel sheet was used in this study; its chemical composition is listed in Table 3-17. Plates 0.7 mm in thickness were cut into strips of size 30×100 mm. The schematic diagram of high strength steel sheet specimen for resistant spot welding was shown in Fig.3-14. The resistance spot welder (FANUC  $\alpha$ 8/4000is type) had been utilized for the experiment is shown in Fig.3-15.

Table 3-17 Material used in RSW process (wt-%)

Material	C	Si	Mn	P	S	Fe
MJSC340D	0.062	0.48	0.95	0.013	0.004	Balance

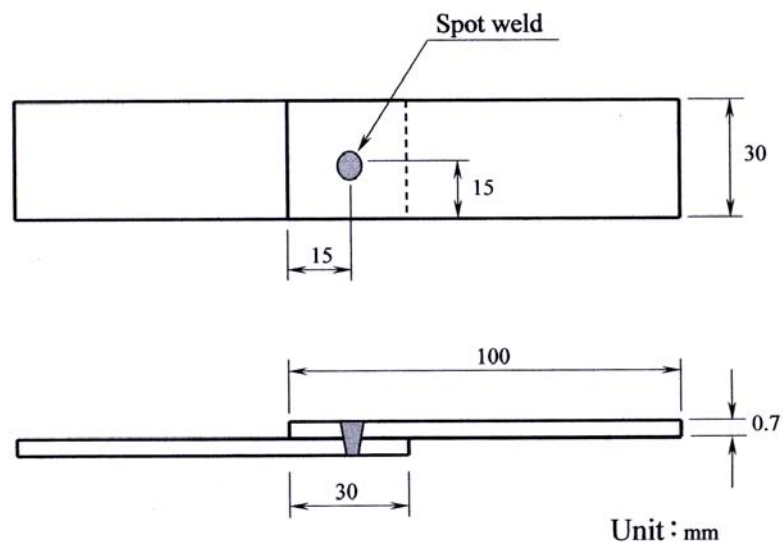


Fig. 3-14 Schematic diagram of the specimens



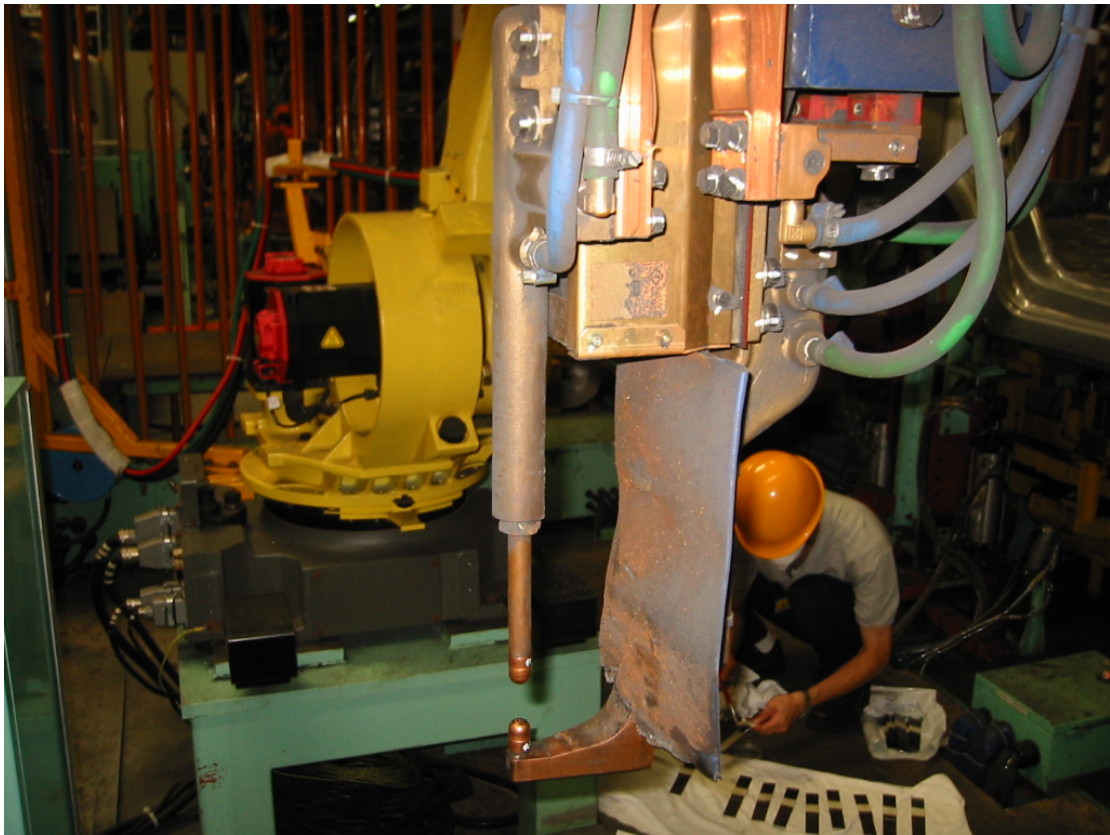


Fig. 3-15 Resistance spot welder and prepared specimens

### ***Control and noise factor of RSW process***

By making reference to the existing parameter conditions in the production line, the range of experimental parameter value has been initially framed as below: welding current 6200 ~ 11000 A, welding time 8 ~ 26 cycles, electrode force 1.8 ~ 3.3 kN and the size of electrode tip  $\phi 3 \sim \phi 6$  mm. The value of each welding process parameter at the different levels is listed in Table 3-18.

Surface condition of the welding area was selected as the noise factor in this study. The specimens at level one (N1), without any cleaning treatment, may have been tarnished with dirt and / or grease. The surface impurities were

removed and the surface cleaned with acetone at level two (N2). The initial conditions of production operation currently were welding current at 7800A, welding time at 8 cycles, electrode force at 1.8 kN and the size of electrode tip at  $\phi 4$  mm.

Table 3-18 Control factors of RSW process

Factor	Process parameter	Level 1	Level 2	Level 3	Level 4
A	The size of electrode tip	$\phi 3$ mm	$\phi 4$ mm	$\phi 5$ mm	$\phi 6$ mm
B	Welding current	6200 A	7800 A	9400 A	11000 A
C	Electrode force	1.8 kN	2.3 kN	2.8 kN	3.3 kN
D	Welding time	8 cycles	14 cycles	20 cycles	26 cycles

### ***Orthogonal array experiment***

Four four-level control factors, in addition to one noise factor, were considered in this investigation. The interaction effect between the welding parameters was not considered. Therefore, there are 12 degrees of freedom owing to the 4 control factors. The degrees of freedom for the OA should be greater than or at least equal to those for the process parameters.  $L_{16}(4^5)$  OA that has 15 degrees of freedom was employed in this study. An experimental layout

with an inner array for control factors and an outer array for a two-level noise factor (N1 and N2) is shown in Table 3-19. Four repetitions ( $y_1, y_2, y_3$  and  $y_4$ ) for each trial are used with this experimental arrangement;  $y_1$  and  $y_2$  are N1 specimens (without cleaning);  $y_3$  and  $y_4$  are N2 specimens (cleaned with acetone). The Max. Load for tensile-shear test specimens are shown in Table 3-20.

**Table 3-19 Experimental layout using an  $L_{16}$  orthogonal array**

Trial no.	Control factor				Noise factor			
	A	B	N1 specimens		N2 specimens			
			C	D	$y_1$	$y_2$	$y_3$	$y_4$
1	1	1	1	1				
2	1	2	2	2				
3	1	3	3	3				
·	·	·	·	·				
15	4	3	2	4				
16	4	4	1	3				

Measure data

Table 3-20 Experiment data in RSW process

Trial no.	Control factors				Max. Load	
	A	B	C	D	Average (kN)	SNR (dB)
1	1	1	1	1	3.317	10.41
2	1	2	2	2	4.098	12.25
3	1	3	3	3	4.105	12.26
4	1	4	4	4	4.392	12.85
5	2	1	2	3	3.299	10.35
6	2	2	1	4	3.758	11.49
7	2	3	4	1	3.950	11.91
8	2	4	3	2	3.855	11.70
9	3	1	3	4	2.622	8.36
10	3	2	4	3	3.735	11.44
11	3	3	1	2	4.168	12.39
12	3	4	2	1	4.083	12.22
13	4	1	4	2	2.318	7.29
14	4	2	3	1	3.572	11.05
15	4	3	2	4	3.637	11.21
16	4	4	1	3	4.139	12.24

Total average of SNR for all trial  $\hat{\eta}$  is 11.213 (dB)

### ***Evaluation of initial optimal condition***

The Max. Load of the specimens as discussed earlier belongs to the higher-is-better quality characteristic. The SNRs, which condense the multiple data points within a trial, depend on the three characteristics LB, NB and HB. The equation for calculating the SNR for HB characteristic is

$$SNR = -10 \log_{10} \left( \frac{1}{n} \sum_{i=1}^n \frac{1}{y_i^2} \right) \quad 3-3$$

where  $n$  is the number of tests in a trial (number of repetitions regardless of noise levels). The value of  $n$  is 4 in this study. The SNRs corresponding to Max. Load value of each trial is shown in Table 3-21. The effect of each welding process parameter on the SNR at different levels can be separated out because the experimental design is orthogonal. The description of the SNR for each level of the welding process parameters is summarized in Table 3-21. Fig.3-16 shows the SNR graph obtained from Table 3-21. Basically, the larger is the SNR, the better the quality characteristic (tensile-shear strength) for the specimens. The initial optimal conditions of the RSW process parameter levels,  $A_1B_4C_1D_3$ , can be determined from Fig. 3-16.

Table 3-21 SNR response table for the Max. Load

Factor	Process parameter	Level 1	Level 2	Level 3	Level 4
A	The size of electrode tip	11.941	11.363	11.101	10.449
B	Welding current	9.102	11.558	11.942	12.252
C	Electrode force	11.634	11.507	10.842	10.871
D	Welding time	11.399	10.905	11.571	10.979

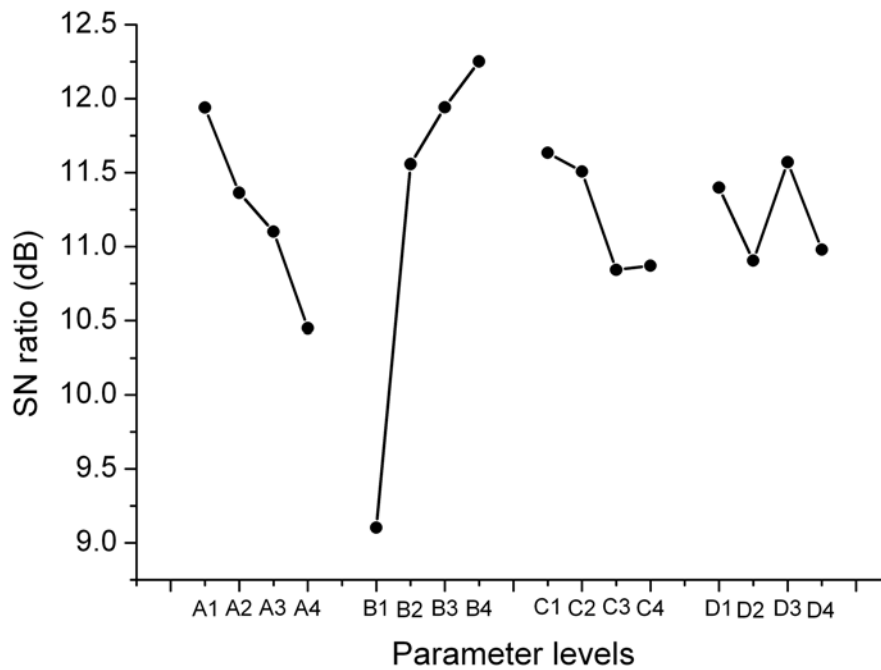


Fig. 3-16 SNR graph for the Max. Load

### *Analysis of variance*

When the contribution of a factor is small, as with factor D (welding time) in Table 3-22, the sum of squares for that factor is combined with the error. This process of disregarding the contribution of a selected factor and subsequently adjusting the contributions of the other factors is known as ‘Pooling’ [9]. The welding current and the size of electrode tip were the significant welding parameters in affecting the quality characteristic, with the welding current being the most significant, as indicated by Table 3-22.

Table 3-22 Results of ANOVA for the Max. Load

Factor	Degree of freedom	Sum of square	Mean square	F- Test	Pure sum of square	Percent contribution
A	3	4.599	1.533	3.42	3.25	9.54%
B	3	24.748	8.249	18.40	23.40	68.61%
C	3	2.071	0.690	1.54	0.73	2.13%
D	3	1.248 *				
Error	3	1.442				
Error (pooled)	(6)	(2.691)	(0.448)		6.15	19.72%
Total	15	34.109			34.229	100%

Mark \* means the factors are treated as pooled error


**Confirmation test and proper regulation**

Refer to Table 3-21 and 3-22, estimated SNR  $\eta_{opt}$  is computed as

$$\eta_{opt} = 11.213 + (11.941 - 11.213) + (12.252 - 11.213) = 12.98 \text{ (dB)}$$

With a CI of 95% for the tensile-shear strength, the  $F_{0.05;1;6} = 5.99$ , and  $V_{ep} = 0.448$ , the sample size for the confirmation experiment  $r$  is 2,  $N = 16$ ,  $DOF_{opt} = 9$ , and the effective sample size  $n_{eff}$  is 1.6. Thus, the CI is computed to be 1.738 (dB). The experimental results (Table 3-23) confirm that the initial optimizations of the RSW process parameters ( $A_{\phi 3\text{mm}}B_{11000A}C_{1.8\text{kN}}D_{20\text{cycles}}$ ) were achieved.

Table 3-23 Confirmation experiment of RSW process



Trial no.	Max. Load				SNR (dB)	Average (kN)	Confidence interval (95%)
	N1 specimens		N2 specimens				
17	4.562	4.505	4.335	4.209	12.861	4.406	12.98 ± 1.74 (dB)
18	4.426	4.343	4.626	4.243	12.875		

Although the conformity of reproducibility for the experimental results has been confirmed with an average Max. Load of specimens as high as up to 4.406 kN obtained; however, a phenomenon of spark taken place between the specimens and the electrode during the spot welding process that leads to a severely shortened life cycle of electrode and an collaterally affected joint



quality of weldment for its subsequent welding. With the ANOVA outcomes (Table 3-22) referenced, a proper regulation of welding current is necessary to cope with the foregoing defects. As learned from Fig. 3-16 (SNR graph), SNR thereof was slightly increased when welding current regulated from 7800A to 11000A, that is, the Max. Load of specimens was not heightened in big magnitude. Therefore, the optimal conditions of parameters obtained from the application of Taguchi Method remained unchanged except the welding current was regulated from 11000A to 7800A. Table 3-24 lists the results of experiment after adjusting the parameters ( $A_{\phi 3\text{mm}}B_{7800\text{A}}C_{1.8\text{kN}}D_{20\text{cycles}}$ ).

Table 3-28 Results of the Taguchi method with proper regulation

Trial no.	Tensile-shear strength				Average (kN)
	N1 specimens		N2 specimens		
19	4.089	3.945	3.926	3.731	3.851
20	3.878	4.041	3.585	3.611	$\left( \begin{array}{l} N1 = 3.988 \\ N2 = 3.713 \end{array} \right)$

### 3.4.2 Real optimization for RSW process

#### *Training of BP network*

A total of 64 input-output data patterns were partitioned into a training set, a testing set and a validating set. Functionally, 60% (38 patterns) were randomly selected for training the neural network while the remaining 20% (13 patterns) were randomly selected for testing and 20% (13 patterns) were randomly

selected for validating. Table 3-25 presents nine options for the NN architecture. After comparing all the data for the MSE value, the structures 5-4-1, 5-5-1, 5-7-1, 5-8-1 and 5-9-1 are the five best convergence criteria. The structure 5-7-1 showed the least simulating error and was therefore selected to obtain a better performance. The topology of the network 5-7-1 with a  $\mu$  value of 0.001 and a  $\theta$  value of 10 is shown in Fig. 3-17.

Table 3-25 Options for different networks in RSW process

Architecture	Mean square error for training	Rank of MSE	Simulating error, % (Compare with average value in Table 3-24)	
			N1 Specimens	N2 Specimens
5-2-1	0.1123			
5-3-1	0.1083			
5-4-1	0.0337	5	-3.81	1.85
5-5-1	0.0282	4	-0.98	6.19
5-6-1	0.2383			
5-7-1	0.0147	2	3.50	-0.54
5-8-1	0.0096	1	-7.92	-6.28
5-9-1	0.0194	3	-4.93	2.36
5-10-1	0.0490			

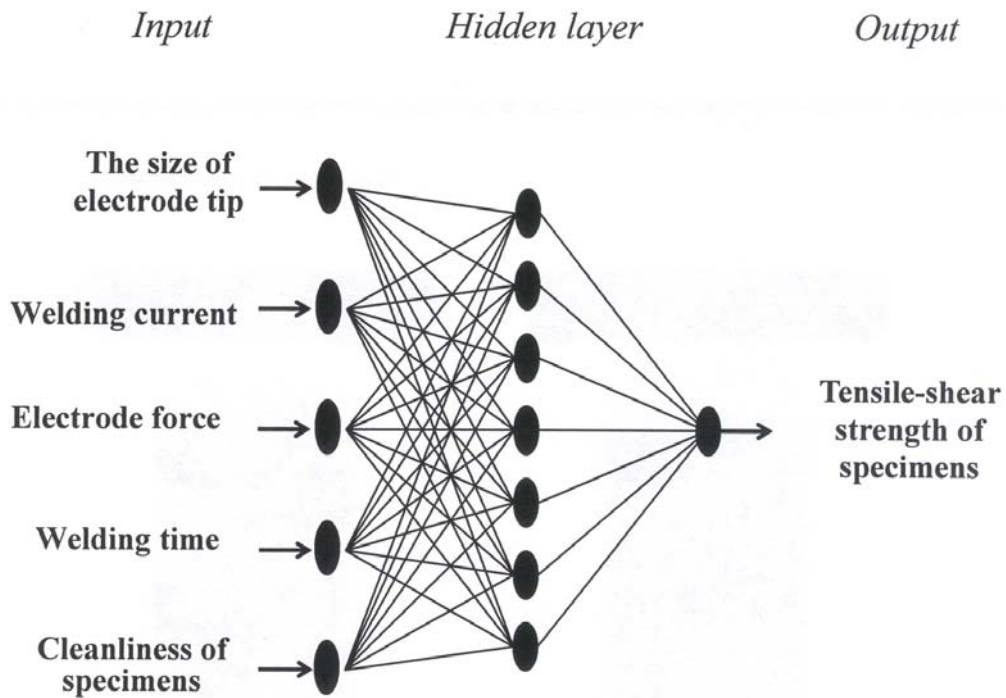


Fig. 3-17 The BP network topology of the RSW process



### ***Simulation with a well-trained network***

The control factor D (welding time) is the insignificant welding parameters in affecting the quality characteristic as shown in Table 3-26. First, the trained network 5-7-1 with 1.47% MSE was employed as the simulating function of the insignificant parameters in this welding process. In Fig. 3-15 ~ 3-18, the N1 specimens (without any cleaning treatment) had simulated with 0 % cleanliness and the N2 specimens (cleaned with acetone) had simulated with 100 % cleanliness.

Fig. 3-18 shows the comparison of simulating results using the factor D (other conditions  $A_{\phi 3\text{mm}}B_{7800A}C_{1.8\text{kN}}$ ), from which it can be seen that the Max. Load of specimens is best for adjusting welding time to 15 cycles.

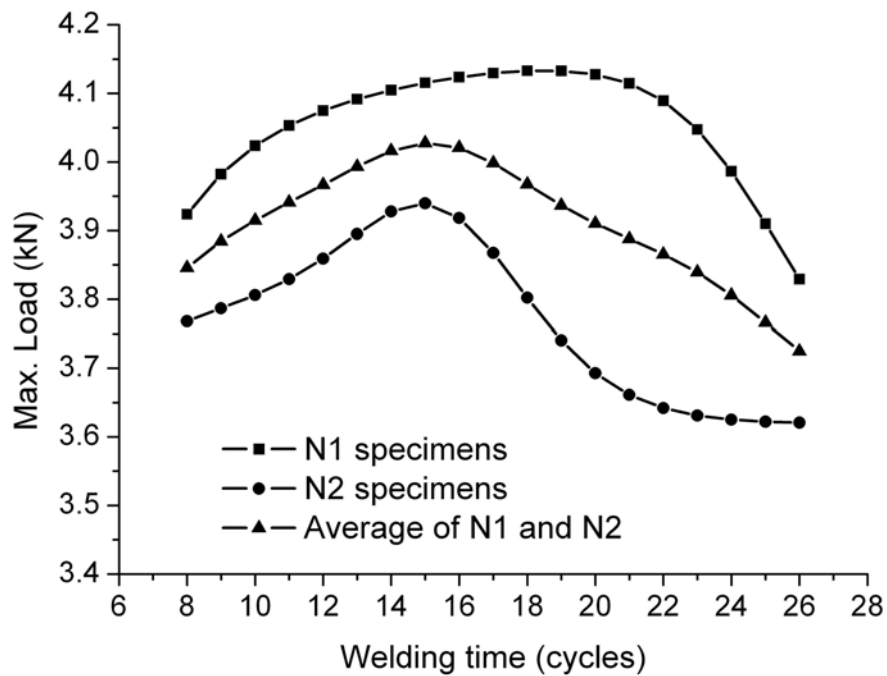


Fig. 3-18 Results of simulating different welding time

Second, Fig.3-19 shows the comparison of simulating results using the factor C (other conditions  $A_{\phi 3\text{mm}}B_{7800A}D_{15\text{cycles}}$ ), from which it can be seen that the Max. Load of specimens is best for setting electrode force at 3.0 kN.

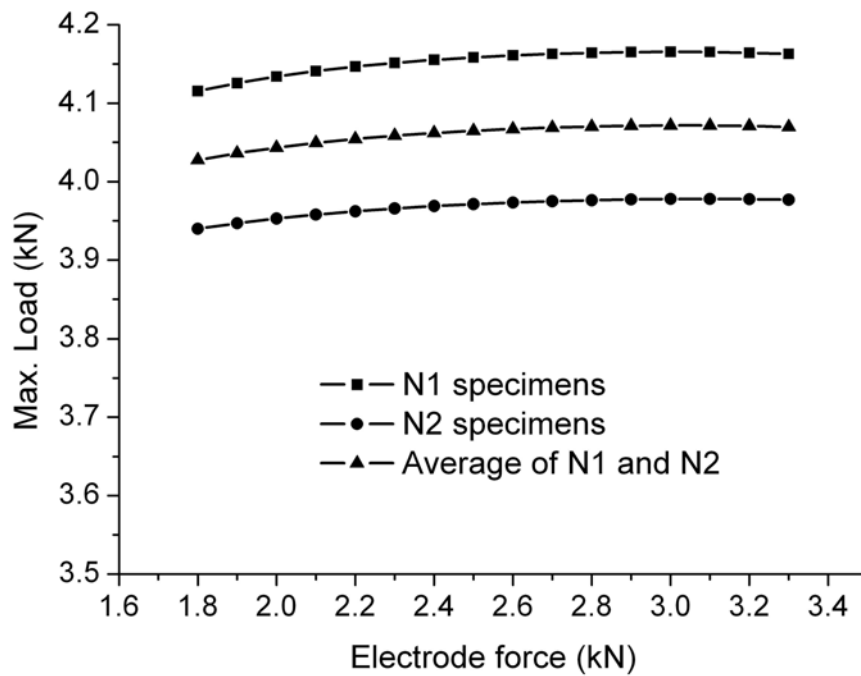


Fig. 3-19 Results of simulating different electrode force

Third, Fig. 3-20 shows the comparison of simulating results using the factor A (other conditions  $B_{7800A}C_{3.0kN}D_{15cycles}$ ), from which it can be seen that the Max. Load of specimens is best for setting the size of the electrode tip at  $\phi 3$  mm.

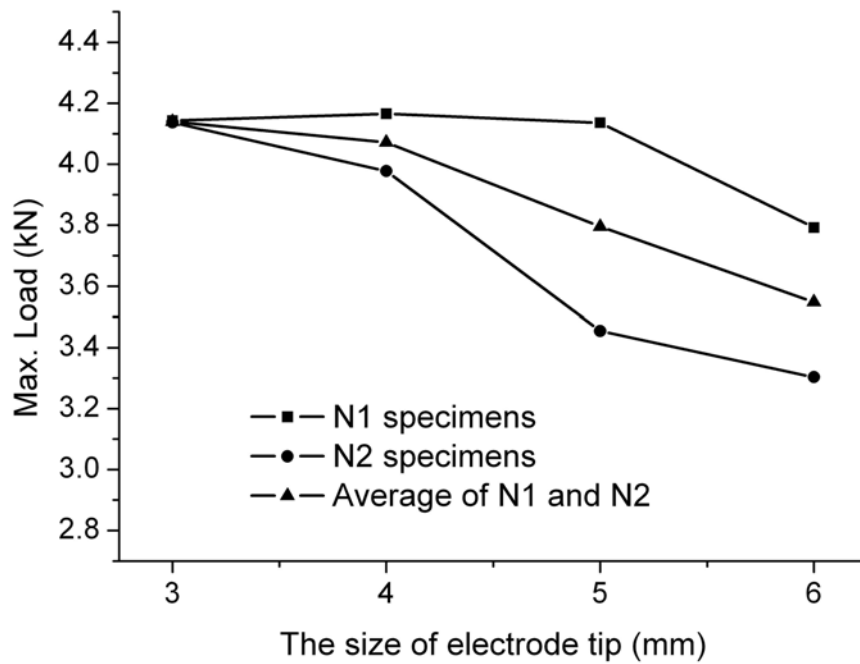


Fig. 3-20 Results of simulating different size of the electrode tip

Finally, Fig. 3-21 shows the comparison of simulating results using the factor B (other conditions  $A_{\phi 3\text{mm}}C_{3.0\text{kN}}D_{15\text{cycles}}$ ), from which it can be seen that welding current and average Max. Load are in direct ratio until about 8200A. The welding current of RSW process for the initial condition is 7800 A. Therefore, the welding current at 7800A has been selected in this study.

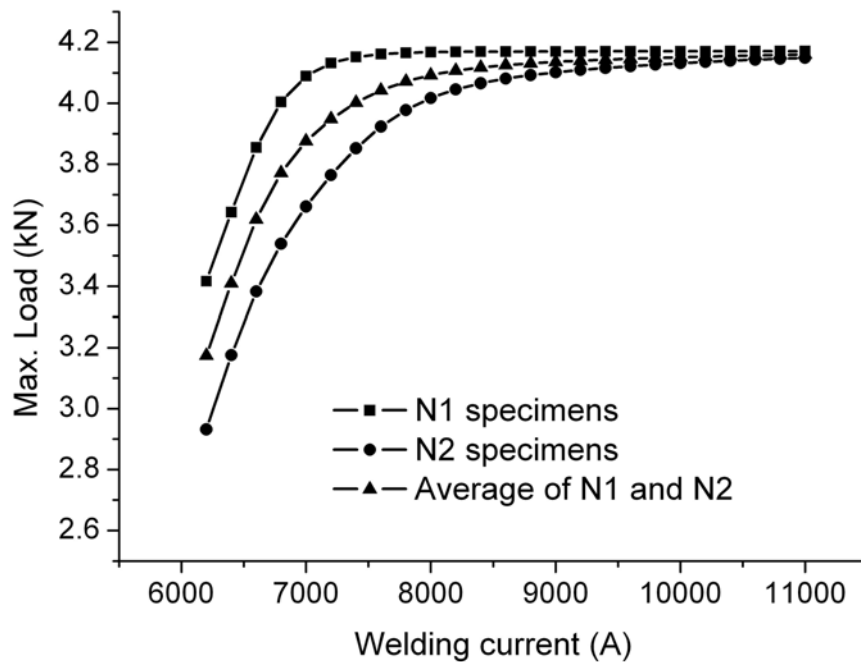


Fig. 3-21 Results of simulating different welding current

# CHAPTER 4

## RESULTS AND DISCUSSION

### 4.1 Experimental results of the GTA welding

By proposed approach, the optimal welding condition of the GTA welding were the electrode size at level 2 ( $\phi 3.2$  mm), the speed of welding torch at level 1 ( $85 \text{ mm min}^{-1}$ ), the arc length at level 3 (2.0 mm), the flow rate of shielding gas at level 1 ( $8 \text{ L min}^{-1}$ ), electrode on 73 degree of angle and welding current on 81 A. Table 4-1 is the experimental results with above optimal welding parameters. In comparing Table 4-1 with 3-7, it is shown that the increase of the average depth-to-width ratio from initial optimal parameters (apply Taguchi method only) to the real optimal parameters (apply Taguchi method and neural network) is 0.12.



Table 4-1 Results of the proposed approach in GTA welding

Trial no.	Depth-to-width ratio				
	N1 specimens		N2 specimens		Average
30	0.780	0.795	0.782	0.792	
31	0.806	0.782	0.773	0.770	



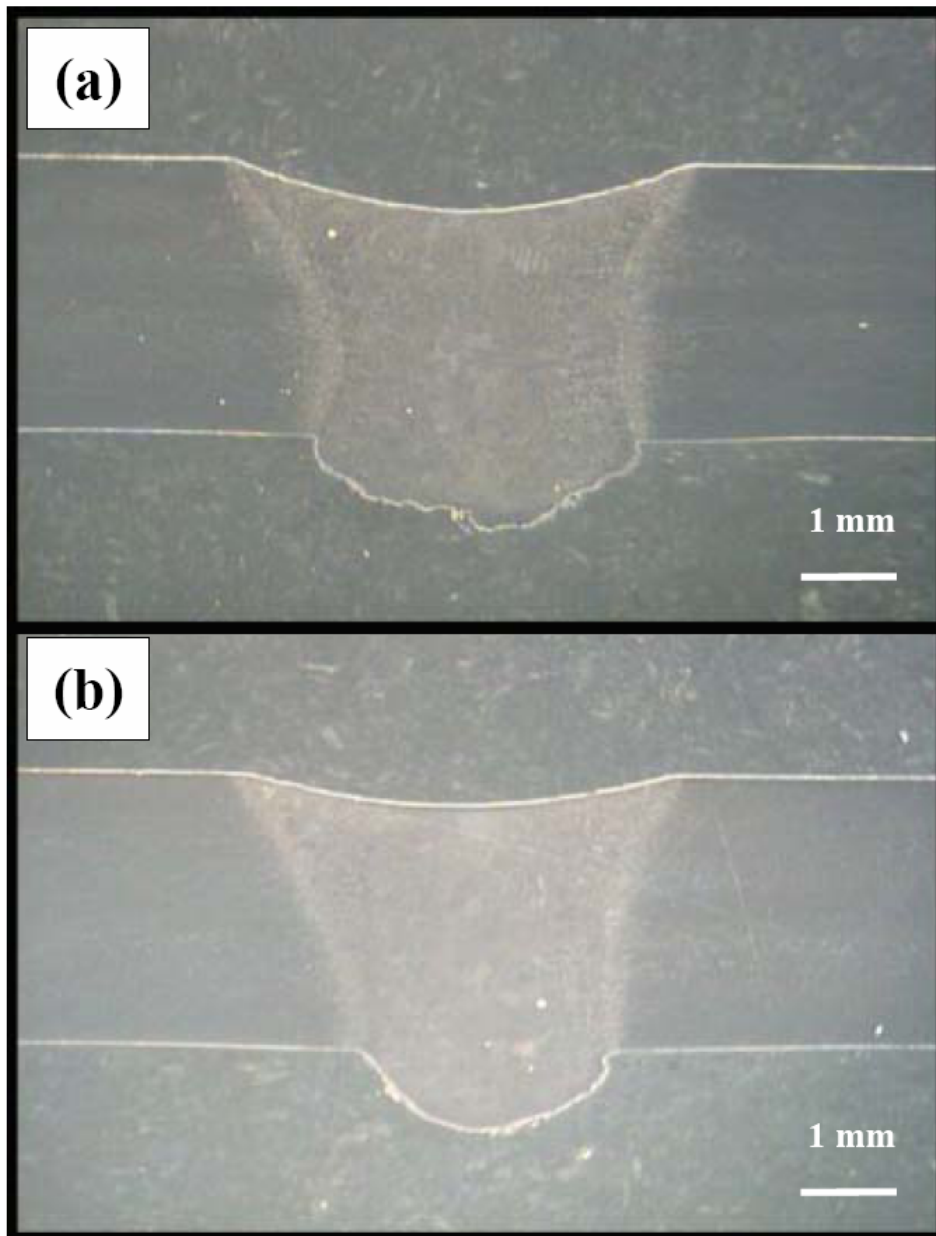


Fig. 4-1 Weld pool geometry for validation

(a) Apply Taguchi method only, DWR = 0.712

(b) Apply proposed approach, DWR = 0.806

The largest weld pool geometry of the initial optimal welding parameters by Taguchi method is 0.712. The largest weld pool geometry of the optimal welding parameters by proposed approach is 0.806. The weld pool geometry of the optimal welding parameters by proposed approach is slenderer than that was applied by the Taguchi method only, as shown in Fig.4-1. In summary, the quality of GTA welding process can be efficiently improved through the proposed approach.

#### 4.2 Experimental results of Nd:YAG laser micro-weld

By combining the Taguchi method and neural networks, the optimal welding condition for Max. Load of the Nd:YAG laser weldment were the focus position on +0.25mm, the pulse peak value on 355 Volt., the pulse frequency on 3.4 pps and the pulse width on 6 msec. Table 4-2 is the experimental results with above optimal welding parameters.

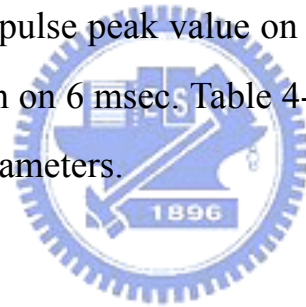


Table 4-2 Results of the proposed approach in laser welding

Trial no.	Max. Load				
	N1 specimens		N2 specimens		Average, kg
29	1.05	1.14	0.94	0.90	
30	1.00	1.07	1.00	0.96	1.013
31	1.10	1.02	0.92	1.05	

In comparing Table 4-2 with 3-15, it is shown that the improvement of the average Max. Load for N2 specimens (without cleaned) from initial optimal parameters to the real optimal parameters is 0.104 kg. The defective rate of the optimal welding parameters with the proposed approach is lower than that with the Taguchi method only, as shown in Table 4-3. In summary, the quality of Nd:YAG laser micro-weld process can be efficiently improved with the proposed approach.

Table 4-3 A comparison of each condition

	Focus position, mm	Pulse peak value, Volt	Pulse width, msec	Pulse frequency, pps	Defective rate, %	Average, kg
Initial condition	0	330	6	2	8.67	0.886
Taguchi method	+0.5	360	6	3	5.37	0.979
Proposed approach	+0.25	355	6	3.4	2.00	1.023

Sample size of comparison: 150

The simulating results obtained with a well-trained neural network model indicate that, the specimens (AA3003 aluminum alloy) with 50% cleanliness contributed most to the Nd:YAG laser micro-weld process. In order to improve the welding quality efficiently, the cleaning treatment to the safety vent and cathode lead of lithium-ion secondary batteries must be corrected.

### 4.3 Experimental results of RSW process

With combination of this Taguchi method and a neural network, the optimal welding conditions for Max. Load with RSW process were electrode tip size at  $\phi 3$  mm, welding current at 7800 A, electrode force at 3.0 kN and welding time at 15 cycles. Table 4-4 shows the experimental results obtained with above optimal welding parameters. Table 4-5 shows the experimental results with the conditions of production operation currently ( $A_{\phi 4\text{mm}}B_{7800\text{A}}C_{1.8\text{kN}}D_{8\text{cycles}}$ ). Comparison of Table 3-24 with Table 4-5 shows that the increase in average Max. Load from the initial conditions to the initial optimal parameters (apply Taguchi method only) is 0.309 kN. Comparison of Table 4-4 with Table 4-5 shows that the increase in average Max. Load from the initial conditions to the real optimal parameters (apply Taguchi method and neural network) is 0.566 kN. The surface condition of specimens for different parameters is shown in Fig.4-2. In summary, the quality of RSW process for high strength steel sheet can be efficiently improved with the proposed approach.

Table 4-4 Results of the proposed approach in RSW process

Trial no.	Max. Load				Average (kN)
	N1 specimens		N2 specimens		
21	4.310	4.169	4.112	3.746	4.108
22	4.153	3.973	4.522	3.876	



Table 4-5 Results of the initial conditions in RSW process

Trial no.	Max. Load				Average (kN)
	N1 specimens		N2 specimens		
23	3.329	3.518	3.605	3.344	3.542
24	3.673	3.575	3.626	3.669	

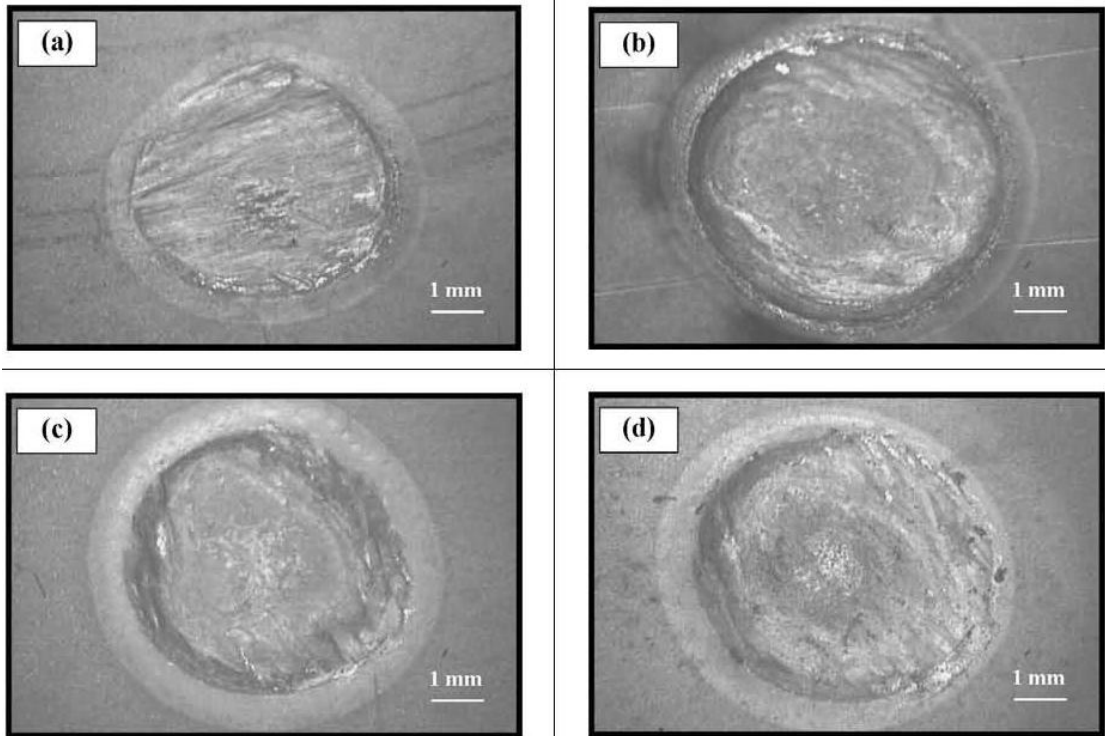


Fig.4-2 Surface conditions of specimens for validation  
(a) Initial conditions  
(b) Apply Taguchi method only  
(c) Apply Taguchi method with proper regulation  
(d) Apply proposed approach

## CHAPTER 5

### CONCLUSION

This dissertation presents an integrated approach of the combination of Taguchi method and neural networks to optimize the process conditions of GTA welding, laser-micro weld and RSW process. Based on the results obtained from this research, the following conclusions can be drawn from this dissertation.

1. In GTA welding process, the improvement of average depth-to-width ratio from initial optimal parameters (apply Taguchi method) to the optimal parameters (apply proposed approach) is about 11.96%. The largest depth-to-width ratio of the initial optimal parameters by Taguchi method is 0.712. The largest depth-to-width ratio of the optimal parameters by proposed approach is 0.806.
2. The ANOVA result indicates that, the electrode angle, welding current, and travel speed are the significant parameters in affecting the depth-to-width ratio of weld pool geometry in GTA welding process.
3. In Nd:YAG laser micro-weld process, The improvement of the defective rate from initial conditions to the initial optimal parameters (apply Taguchi method) is 3.30%; from initial conditions to the optimal parameters (apply proposed approach) is 6.67 %.
4. The simulating results indicate that, the specimens (AA3003 aluminum alloy) with 50% cleanliness contributed most to the Nd:YAG laser micro-weld process. In order to improve the welding quality efficiently, the cleaning treatment to the safety vent and cathode lead of lithium-ion secondary batteries must be corrected.

5. In RSW process, the improvement of the average tensile-shear strength from initial conditions to the initial optimal parameters (apply Taguchi method) is about 8.72%. The improvement from initial conditions to the optimal parameters (apply proposed approach) is about 15.98%.
6. The ANOVA result indicates that, the size of electrode tip and welding current were the significant parameters in affecting the tensile-shear strength in RSW process for high strength steel sheet.
7. Compare with the results of ANOVA, there are 26.88% of error contribution in GTA welding, 7.75% of error contribution in Nd:YAG laser micro-weld process, and 19.72% of error contribution in RSW process. It shows that the experimental error of Nd:YAG laser micro-weld process is least and GTA welding is largest.
8. From the results of confirmation test in these welding processes, the conformity of reproducibility for the experimental results has been confirmed
9. The proposed approach is relatively effective and ease for engineers to apply to a range of other processes. The LMBP algorithm neural network is easy-and-quick to explore a nonlinear multivariate relationship between parameters and responses. It was proved successfully and effectively in this study.
10. In addition, applying the proposed approach allows engineers to directly use neural network software to optimize the parameters without any theoretical knowledge of neural computing.



## REFERENCE

1. H.B. Cary, Modern Welding Technology, Prentice-Hall, New Jersey, 1994.
2. G. Taguchi, E.A. Elsayed and T.C. Hsiang, Quality Engineering in Production Systems, McGraw-Hill, New York, 1989.
3. C.T. Su, C.C. Chiu, and H.H. Chang, “Parameter design optimization via neural network and genetic algorithm”, *Int. J. Ind. Eng.*, **7**(3), 224-231, 2000.
4. I.S. Kim, Y.J. Jeong, and C.W. Lee, “Prediction of welding parameters for pipeline welding using an intelligent system”, *Int. J. Adv. Manuf. Technol.*, **22**, 713-719, 2003.
5. H.K.D.H. Bhadeshia, D.J.C. Mackay, and L.E. Svensson, *Mater. Sci. Technol.*, **11**, 1046-1051, 1995.
6. John F.C. Khaw, B.S. Lim, and Lennie E.N. Lim, “Optimal design of neural networks using Taguchi method”, *Neurocomputing*, **7**, 225-245, 1995.
7. P.J. Ross, Taguchi Techniques for Quality Engineering, McGraw-Hill, New York, 1988.
8. G. Taguchi, Taguchi methods: Design of Experiments, American Supplier Institute, Inc, Michigan, 1993.
9. R.K. Roy, A primer on the Taguchi Method, Van Norstrand Reinhold, New York, 1990.
10. M.S. Phadke, Quality Engineering using Robust Design, Prentice-Hall, New Jersey, 1989.
11. S.C. Juang and Y.S. Tarn, “Process parameter selection for optimizing the pool geometry in the tungsten inert gas welding of stainless steel”, *J. Mater. Process. Technol.*, **122**, 33-37, 2002.
12. Wei Li, S. Jack Hu, and Shao-Wei Cheng, “Robust design and analysis for manufacturing processes with parameter interdependency”, *Manuf. Syst.*,

- 21(2)**, 93-100, 2002.
- 13.Y.S. Tarng, S.C. Juang and C.H. Chang, “ The use of grey-based Taguchi methods to determine submerged arc welding process parameters in hardfacing”, *J. Mater. Process. Technol.*, **128**, 1-6, 2002.
- 14.C.T. Su, and T.L. Chiang, “Optimizing the IC wire bonding process using a neural networks/genetic algorithms approach”, *J. Intell. Manuf.*, **14**, 229-238, 2003.
- 15.D.W. Coit, B.T. Jacson, and A.E. Smith, “Static neural network process model: considerations and cases studies”, *Int. J. Prod. Res.*, **36(11)**, 2953-2967, 1998.
- 16.K. Funahashi, “ On the approximate realization of continuous mapping by neural network”, *Neural Netw.*, **2**, 183-192, 1989.
- 17.M.T. Hagan, H. Demuth and M. Beale, Neural Network Design, PWS Publishing co., Boston, 1996.
- 18.M.T. Hagan and M.B. Menhaj, “ Training feedforward networks with the Marquardt algorithm”, *IEEE Trans, Neural Netw.* , **5(6)**, 989-993, 1994.
- 19.F. A. Dias, A. Antunes, J. Vieira and A. Mota, “ A sliding window solution for the on-line implementation of the Levenberg-Marquardt algorithm”, *Engineering Applications of Artificial Intelligence*, **19**, 1-7, 2006.
- 20.K. Kumar and M.A. Alsaleh, “ A comparative study for the estimation of parameters in nonlinear models”, *Applied Mathematics and Computation* **77**, 179-183, 1996.
- 21.S. Haykin, Neural Networks-A Comprehensive Foundation, Macmillan College Publishing co., New York, 1994.
- 22.H. Demuth and M. Beale, Neural Network Toolbox-For use with MATLAB, The Math Works, Inc., Boston, 1998.

- 23.I.S. Kim, I.S. Son, C.E. Park, I.J. Kim and H.H. Kim, “ An investigation into an intelligent system for predicting bead geometry in GMA welding process”, *J. Mater. Process. Technol.*, **159**, 113-118, 2005.
- 24.C.S. Wu, T. Polte and D. Rehfeldt, “ Gas metal arc welding process monitoring and quality evaluation using neural networks”, *Sci. Technol. Weld Joi.* , **5**(5), 324-328, 2000.
- 25.D.S. Nagesh and G.L. Datta, “ Prediction of weld bead geometry and penetration in shielded metal-arc welding using artificial neural networks”, *J. Mater. Process. Technol.*, **123**, 303-312, 2002.
- 26.G.E. Ridings, R. C. Thomson and G. Thewlis, “ Prediction of multiwire submerged arc weld bead shape using neural network modelling”, *Sci. Technol. Weld Joi.*, **7**(5), 265-279, 2002.
- 27.J.Y. Jeng, T.F. Mau and S.M. Leu, “ Prediction of laser butt joint welding parameters using back propagation and learning vector quantization networks”, *J. Mater. Process. Technol.*, **99**, 207-218, 2000.
- 28.J.I. Lee and K.W. Um. Tarnq, “ A prediction of welding process parameters by prediction of back-bead geometry”, *J. Mater. Process. Technol.*, **108**, 106-113, 2000.
- 29.J.M. Vitek, S.A. David, M.W. Richey, J. Biffin, N.Blundell and C.J. Page, “ Weld pool shape prediction in plasma augmented laser welded steel”, *Sci. Technol. Weld Joi.*, **6**(5), 305-314, 2001.
- 30.Y.S. Tarnq, H.L. Tsai and S.S. Yeh, “ Modeling, optimization and classification of weld quality in tungsten inert gas welding”, *Int. J. Machi. Tools & Manuf.*, **39**, 1427-1438, 1999.
- 31.Y.L. Han, “ Artificial neural network technology as a method to evaluate the fatigue life of weldments with welding defects”, *Int. J. Pres. Ves. & Piping*,

- 63, 205-209, 1995.
- 32.H. Rowlands, M.S. Packianather and E. Oztemel, “ Using artificial neural networks for experimental design in off-line quality”, *Journal of Systems Engineering*, 6, 46-59, 1996.
- 33.C.C. Chiu, C.T. Su, G.H. Yang, J.S. Huang, S. C. Chen and N.T. Cheng, “Selection of optimal parameters in gas-assisted injection moulding using a neural network model and the Taguchi method”, *Int. J. Quality Sci.*, 2, 106-120, 1997.
- 34.J. Norrish, Advanced Welding Processes, IOP Publishing Ltd., New York, 1992.
- 35.S.C. Juang and Y.S. Tarn, “ Process parameter selection for optimizing the pool geometry in the tungsten inert gas welding of stainless steel”, *J. Mater. Process. Technol.*, 122, 33-37, 2002.
- 36.Paulo J. Modenesi, Eustaquio R. Apolinario and Iaci M. Pereira, *J. Mater. Process. Technol.*, 99, 260-265, 2000.
- 37.Walter W. Duley, Laser Welding, John Wiley & Sons, Inc., New York, 1998.
- 38.Christopher Dawes, Laser Welding, McGraw-Hill Inc., New York, 1992.
- 39.L.K. Pan, C.C. Wang, Y.C. Hsiao and K.C. Ho, “ Optimization of Nd:YAG laser welding onto magnesium alloy via Taguchi method”, *Opt. Laser Technol.*, 37, 33-42, 2004.
- 40.J.M. Jr. Sawhill and J.C. Baker, “Spot weldability of high-strength sheet steel”, *Weld. J.*, 59(1), 19-s to 30-s, 1980.
- 41.Z. Han, J.E. Indacochea, C.H. Chen and S. Bhat, “ Weld nugget development and integrity in resistance spot welding of high-strength cold-rolled sheet steels”, *Weld. J.*, 1993, 72(5), 209-s to 216-s.
- 42.W.F. Savage, E.F. Nippes and F.A. Wassell, “Dynamic contact resistance of

series spot welds”, *Weld. J.*, 1978, **57**(2), 43-s to 50-s.

43. Yu Thomas, Study on the Pulse Nd:YAG laser welding for packaging process parameters, National Tsing Hua University (Taiwan), Thesis, 2002.



# AUTHOR'S PUBLICATION LIST

## A. Referred Papers

1. H. L. Lin and C. P. Chou., Optimisation of the GTA welding process using Taguchi method and a neural network, *Science and Technology of Welding and Joining*, 2006, 11(1), 120-126.
2. H. L. Lin and C. P. Chou., Modeling and optimization of Nd:YAG laser micro-weld process using Taguchi Method and a neural network, Accepted to *International Journal of Advanced Manufacturing Technology*, 2006.
3. H. L. Lin, Ting Chou and C. P. Chou., Optimization of resistance spot welding process using Taguchi Method and a neural network, Accepted to *Experimental Techniques*, 2006.
4. H. L. Lin, Ting Chou and C. P. Chou., "Modeling and optimization of the resistance spot welding process in automobile industry," Submitted to *Proceedings of the Institution of Mechanical Engineers Part D Journal of Automobile Engineering*, Under review, 2006.
5. 林玄良、周長彬，Nd:YAG 雷射銲接穩健性製程設計之研究，銲接與切割，15(4)，PP.56-61，2005。
6. 林玄良、周定、周長彬，建立汽車鋼板接合參數預測模型之研究，銲接與切割，16(1)，PP.56-61，2006。

## B. Conference Papers

1. H. L. Lin and C. P. Chou, Modeling and Optimization of resistance spot welding process in automobile industry, The First South-East Asia - International Institute of Welding Congress, Bangkok, Thailand, 21-22 November 2006.

2. H. L. Lin, C. P. Chou, and M. S. Chen, Selection of the GTAW-flux process parameters on type 310 stainless steel via a Taguchi-Neural approach, Abstract of paper has been accepted to The International Welding/Joining Conference, Seoul, Korea, 10-12 May 2007.
3. 林玄良、蔡勝禮、周長彬，雷射微接合製程參數最佳化之實務研究，中華民國銲接協會九十二年會，高雄，2003.10。
4. 林玄良、周長彬，汽車鋼板電阻點銲參數最佳化之研究，中華民國第八屆車輛工程學術研討會，台北，2003.10。
5. 林玄良、周長彬，不銹鋼薄板銲接製程參數最佳化之研究，中國機械工程學會第二十屆全國學術研討會，台北，2003.12。
6. 林玄良、周長彬，應用類神經網路於雷射微接合製程之研究，中華民國銲接協會九十三年會，台北，2004.10。
7. 林玄良、周長彬，應用田口方法與類神經網路於 TIG 銲接製程之研究，中國工業工程學會九十三年會，台南，2004.12。
8. 林玄良、周定、周長彬，不銹鋼 TIG 銲件提昇銲道深寬比之研究，台灣銲接協會九十四年會，彰化，2005.10。
9. 周定、林玄良、周長彬，田口方法在汽車鋼板接合參數最佳化之應用，台灣銲接協會九十四年會，彰化，2005.10。
10. 林玄良、周長彬，提昇雷射微接合銲件製程品質之研究，中國工業工程學會九十四年會，新竹，2005.12。
11. 林玄良、陳明松、黃泰勳、周長彬，低碳鋼與不銹鋼 TIG-Flux 對接製程之參數研究，台灣銲接協會九十五年會，高雄，2006.10。
12. 林玄良、周定、周長彬，車身用高張力鋼板接合製程之參數研究，中華民國第十一屆車輛工程學術研討會，彰化，2006.11。



## C. Others

1. 林玄良，探討田口方法在自動化銲接之應用，銲接與切割，11(2)，pp.35-38，2001。
2. 林玄良，應用田口方法改善工程中的品質問題，機械技術雜誌，195，pp.146-150，2001。
3. 林玄良，遺傳演算法在銲接工程之應用，銲接與切割，11(6)，pp.14-18，2001。
4. 林玄良，淺談汽車用鋁合金及其最新鑄造技術，機械技術雜誌，200，pp.137-139，2001。
5. 林玄良，雷射銲接在汽車工業的最新應用，機械技術雜誌，206，pp.147-152，2002。
6. 林玄良，淺談鋁合金半固態成形技術，機械技術雜誌，210，pp.124-127，2002。
7. 林玄良，淺談摩擦攪拌銲接技術及其最新發展，機械技術雜誌，210，pp.148-152，2002。
8. 林玄良，銲接製程之可靠度分析，銲接與切割，12(4)，PP.31-40，2002。
9. 林玄良，電漿電弧銲接在微接合加工技術之應用，機械技術雜誌，216，pp.113-117，2003。
10. 林玄良，銲接對壓力容器的影響及問題對策，工業安全衛生月刊，164，pp.32-40，2003。
11. 周長彬、林玄良、黃處明、潘聖富，高熵合金銲接性能研究結案報告，工業技術研究院分包學術機構研究計畫，新竹，2003.12。